Design of an Instrumented Handle for Determining Forces Involved in Surgical Cutting

A thesis

submitted by:

Nathaniel L. Britton

In partial fulfillment of the requirements
for the degree of

Master of Science

in

Mechanical Engineering

TUFTS UNIVERSITY

February 2011

Advisor:

Professor Gary G. Leisk, Ph.D.

Acknowledgements

First, I am heartily thankful to my advisor Gary G. Leisk, Ph.D., whose guidance, support and encouragement helped me with this project. Secondly, I would like to thank my family and friends, especially my parents, for their high level of continued support over the years. I would also like to thank my committee members, Anil Sigal, Ph.D. and Brian Woytowich, for their assistance along the way and for agreeing to serve on my thesis committee. I would like to thank Tufts University and the Mechanical Engineering Department for making me a better engineer. Last but not least, I would especially want to thank James O'Leary, who started me on this journey. In my appreciation, I would like to commemorate this project in his honor for all his support.

Table of Contents

List of Figures

List of Tables

Abstract

One of the most important tools a surgeon uses in surgical procedures is surgical blades. To provide insight into the act of cutting tissue, improve the quality of surgical blades, and generate critical data necessary for creating realistic physical and virtual training environments, it is critical to have good understanding of the biomechanical properties of tissues and the forces needed to cut tissue. In this project, a novel device consisting of a strain gauge-based force transducer mounted within a typical scalpel-style handle was designed and fabricated to quantitatively measure the forces (stabbing, cutting, and lateral forces) applied to surgical blades during a cutting operation. The evaluation of the device focused on the accuracy and repeatability of force measurement. Two surgical blades (Becton Dickinson #376500 and 376700) and two different mediums (Dragon Skin® and porcine loin) were tested. The evaluation has shown that forces involved in the stab and cut direction can be accurately measured with this device and the resolution and repeatability are high enough to differentiate the forces exerted between several blades interacting with different mediums. Future modifications to the instrumented tool are envisioned, with the goal of improving measurements in the stab direction, implementing on-board electronics for tetherless operation, and allowing for *in-vivo* testing.

1. Introduction

Surgical practice influences the design of medical instrumentation. In the hospital, surgeons perform operations with the aid of medical instruments (e.g., surgical tools, surgical blades). The development of new instrumentation is largely driven by continuously improving surgical techniques. As the surgical requirements of surgeons change, new technologies need to be developed to improve the quality of current surgical instruments. New medical instrumentation needs to be developed to meet the increased demands for higher performance and precision as well as the increased desire for minimally invasive techniques. Surgeons provide feedback on their experience with current instruments and specify desired effects during post-surgery healing. With surgeons input, manufacturers must improve their current instruments and develop new instruments to satisfy these ever-changing needs.

One of the most important tools a surgeon uses in surgical procedures is surgical blades. Surgical blades have been designed to cut particular tissue in specialized procedures (e.g., arthroscopic, vascular, or eye surgery). In the case of ophthalmic surgery, ophthalmic blades are designed to cut cornea and sclera tissue using minimal applied forces. Therefore, the surgical blade's sharpness and geometry is determined based on the tissue in which the blade is cutting and the surgical operation. To improve quality of surgical blades, it is important to gain additional understanding of biomechanical properties of tissue and cutting forces required to cut tissue.

To understand these tissue properties, tissue properties must be studied quantitatively. *In-vivo* testing methods conducted within the body would be an ideal method to determine different tissue's biomechanical properties and the cutting force required to operate on tissues. It is well known that surgical instruments are best suited for a specific tissue, tissue structure and/or surgery type; however, this assessment is based on the surgeons' subjective experience. In fact, relatively little quantitative data exists in how surgical instrumentation interacts with *in-vivo* tissue. Thus, quantitative measures may inform the development of new technologies rather than relying on subjective observation alone. Using quantitative measurement techniques would ensure that the development of the new instrumentation would meet all design requirements.

Determining the interaction forces between instrument and tissue would expand the capabilities of surgical simulation. Recently, systems have been developed to simulate the cutting of tissue *in-vivo*. Simulation-based training systems have been used to model operational conditions without the need for a patient. In these training environments, the training system simulates the tissue response as surgeons practice their surgical procedures. A resistance force, representative of tool interaction with the particular tissue, is applied to the simulation instrument which feeds back to hand-held system tools. In this way, the simulation procedure mimics the experience of using cutting tools during an actual operation. However, the force feedback requires knowledge of the applied forces of the medical instrument during an actual operation. By studying and understanding biomechanical properties of tissue and cutting of tissue, the correct

applied force can be incorporated into the simulation for each tissue and tissue structure and would make the training experience more effective and life-like [1].

Like the simulation procedures, *in-vivo* procedures involving the removal of tissue (e.g., tumor resection) need accurate measurements of forces and material properties. In the case of navigational systems, the procedures rely heavily upon prediction of future events; therefore, knowledge about material properties is necessary. A surgical navigational system that involves a Finite Element Analysis (FEA) modeling tool uses the ever-changing images from an imaging modality (e.g., magnetic resonance imaging, MRI) and a library of biomechanical tissue properties to compute the tissue deformation for the doctor to help in the ongoing surgical procedure. Without this information concerning material properties, the surgical procedures would be much riskier. For example, when removing cancerous cells from a brain, the brain structure deforms and changes shape, making it difficult to determine the movement of the cancerous structure and remove the cancer cells sufficiently. The research team at the Massachusetts Institute of Technology (MIT) has developed a technique, to determine the biomechanical properties of soft tissue with an *in-vivo* non-destructive test. This method aims to understand the components of a selected soft tissue. This technique will aid in the development of the FEA portion of the navigational system to remove brain cancer cells [2].

Micro-Electro-Mechanical System (MEMS) devices have a potential application in the surgical world primarily in repair and/ or removing tissue. By introduces a MEMS device into the body to aid in the repair and/or removal of

damaged or problem tissue, such as a torn vein or cancer cells, this could increase patient recovery. To perform these actions the MEMS devices require two part apparatus: repair/ removal and stability support. The repair/ remove apparatus performs the operation of removing the tissue and stability support allows secure attachment to a nearby tissue during the operation. Understanding the biomechanical properties of cutting tissue would enable proper repair without causing damage to surrounding tissues [3].

Current research employs *in-vitro* test methods for assessing biomechanical properties of tissue (e.g., modulus of elasticity, etc.). With some modifications to testing equipment, these research areas could become *in-vivo* test instruments. The data generated from *in-vivo* test instruments would produce a database in which the data could be used in the future for a variety of purposes. Two test methods that could be modified are discussed. One research group uses a custom design transducer instrument to measure the force needed to puncture the liver and spleen; two structures with different levels of elastin (i.e., low for liver and high for spleen). In addition, the research group was able to measure the surface displacement before puncturing these structures [4]. Instead of the puncture force, another research group used a custom designed transducer table-top instrument to measure the cutting forces by tracking the blade through the medium [5]. The limitations to this instrument are that it only measures cutting force, is large in size, and its lack of flexibility for different applications. Even though these *in-vitro* methods are successful, modifications could allow the test equipment to be brought in the operating room to allow *in-vivo* testing. For

example, potential modifications may include reducing the instrumentation size into a hand-held device, increasing capability, minimizing measurement error, enhancing measurement accuracy, and changing the medical grade material or sterilization method.

Research groups are beginning to understand the interaction between instruments and *in-vivo* tissue. A soft tissue database is being constructed using data about tissue properties gathered from *in-vitro* and *in-vivo* test methods. One group in the Department of Surgery at the University of California, San Francisco, and Robotics and Intelligent Machines Laboratory at University of California, Berkeley has been using test instruments to generate various measurements of soft tissue. The research group measured the tissue-instrument interaction using surgical instruments with force sensors and has created a database of soft tissue properties [6]. However, other groups should confirm and extend the database using other measurements.

Measurements of the forces acting on a blade when cutting are of particular importance. The loading conditions applied to a surgical blade while in operation include stabbing, cutting, and lateral forces, as well as, associated torque values. A three dimensional representation of stab, cut and lateral forces and their applied direction are illustrated in Figure 1.

A. Direction of stabbing force towards blade occurring along shaft (Red arrows)

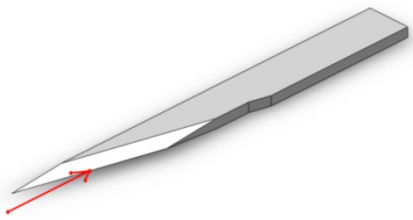

B. Direction of cutting force perpendicular to blade (Green arrows)

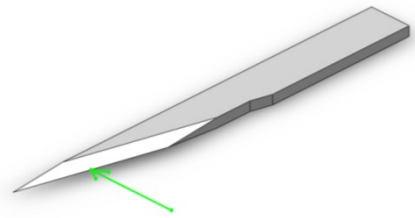

C. Direction of lateral movement force perpendicular to blade (Blue arrows)

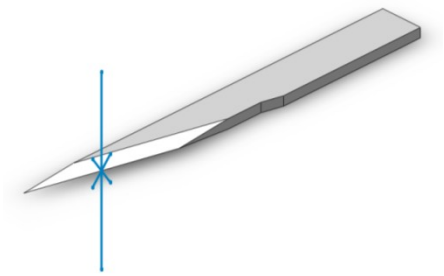

D. Stabbing (Red arrows), cutting force (Green arrows), and lateral Movement Force (Blue arrows)

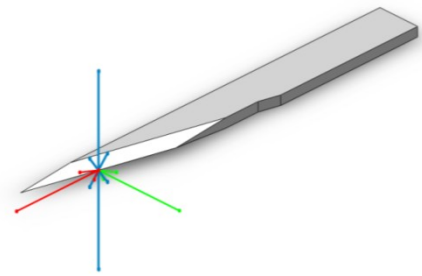

Figure 1: Directional Forces on a Blade when Cutting.

The stabbing force is the applied force exerted on a blade that is directed towards and along the shaft of the surgical blade, shown in Figure 1-A. The cutting force is the applied force on to a blade that is directed toward the surgical blade's cutting edge and acts perpendicular to the shaft and stabbing force, shown in Figure 1-B. The lateral force is the applied force on a blade which is perpendicular to both the stabbing and cutting forces, shown in Figure 1-C. Unlike the stabbing and cutting forces, which only have one component, the lateral force has two opposing components directed towards the surgical blade. Thus, the resultant lateral force changes based on which side of the surgical blade

the force is applied. Torsional loading acts to twist the blade around the blade and shank.

The ultimate goal of this project was to develop and evaluate a new prototype instrument (identified as the Instrumented Handle) for measuring cutting forces, which would eventually be used in an *in-vivo* environment. The approach described involves the development of an initial prototype that has been evaluated under *in-vitro* conditions. The test instrument's principal function is to aid in the understanding of cutting by measuring the force generated from the interaction between a surgical blade and tissue during an operation. Thus, the Instrumented Handle employs transducer and strain gage technology to examine the forces involved when cutting *in-vitro* tissue. The Instrumented Handle was a custom designed surgical handle in which a surgical blade would be mounted during an operation. The experimental design was evaluated for accuracy, repeatability, and reliable measurement using two different types of blades and two different mediums. If successful, the instrument system design and system concept may have greater utility and be used to evaluate different surgical blades/needles in a variety of surgical procedures, both *in-vitro* and *in-vivo*.

2. Design

A multi-use device was designed to quantitatively measure the stabbing, cutting, and lateral forces applied to surgical blades used for surgery. Any applied torque loading is considered negligible for this project.

The design consisted of several elements, including an Instrumented Handle, Measurement System, and Test System. The Instrumented Handle consisted of the blade holder, transducer, and sleeve to protect the transducer and to allow the user to easily hold the instrument. The Measurement System element was integrated into the Instrumented Handle transducer element. These elements acting together would measure the applied force acting on the surgical blade during the cutting operation. The external Test System element directly communicated with the Instrumented Handle to record data.

2.1. Instrumented Handle

An Instrumented Handle was created to measure stabbing, cutting and lateral force on a surgical blade when cutting tissue. The key design element is a strain gage-based transducer mounted inside the handle. This transducer allows precise measurement of strain, which is then converted mathematically into force. The strain gages measure the deformation of an object (i.e., measuring the strain of the object). Strain, , is related to the modulus of elasticity, E, and stress, , based on equation 1. Furthermore, stress is directly related to force and body geometry. Designing a custom transducer element allows the forces involved in surgical cutting operation to be determined.

– **(1)**

The Instrumented Handle design is shown in Figure 2-A. The handle consists of several components: a transducer apparatus that has strain gages mounted at critical locations, a sleeve, and a terminal junction.

A. Instrumented Handle

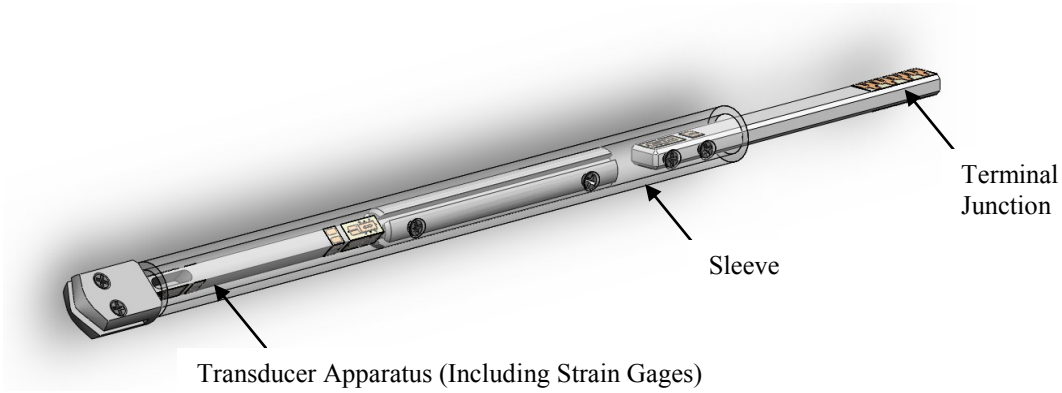

B. Transducer Apparatus

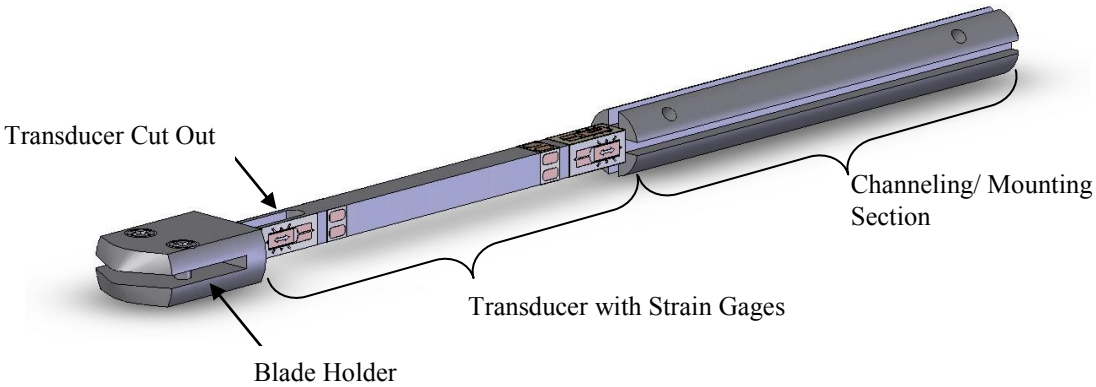

Figure 2: Instrumented Handle & Components.

Within the transducer apparatus, a transducer element, strain gages, blade holder, and channeling/mounting section serve various functions, as shown in Figure 2-B. The function of the transducer element is to translate and amplify applied force into material strain. The strain gages, mounted in intimate contact with the apparatus, convert the detected strain into resistance change, which can

be used to infer the level of applied force. Both the design of the transducer element and strain gages will be discussed in further detail later in this section. The blade holder keeps the surgical blade in the proper location while performing an operation. Furthermore, the channeling/ mounting section of the transducer apparatus directs the wiring of the strain gages back through the sleeve to the terminal junction. The terminal junction is a plate of electrical terminals in which wire connections from the strain gages and computer are made. These wires are mounted at this location to ensure the wires would remain connected to the strain gages and the computer. The blade holder, transducer, and channeling/ mounting section are connected together through a one-piece design, manufactured with 316 stainless steel. The use of stainless steel in constructing the transducer apparatus enabled the design to be small, more compact, and robust, reducing the size of components and consideration of multi-use sterilization method requirements. The sleeve is a hollow tube that encases the transducer element and becomes the handle of the Instrumented Handle. The tubular design of the sleeve protects the transducer element and strain gages from outside interference (e.g., applying undesired bearing loading from operator handling, contaminants that would damage the strain gages, etc.). This sleeve is attached to the channeling/ mounting section of the transducer apparatus and to the terminal plate with several screws.

2.1.1. Transducer Design

The transducer, shown in Figure 2 and Figure 4, combines several key design elements. Taking advantage of beam theory and design, the transducer

uses beam-style construction. The transducer beam resembles a solid, square cross-section cantilever beam with the free end acting as the blade holder and the fixed end consisting of the channeling/ mounting section of the transducer apparatus. In beam theory, there is theoretically a plane that spans the length of the beam, located at a specific height in the beam where no strain occurs. This plane, known as the neutral plane, is located at the mid-height level of a square cross-section beam. By design, the symmetric transducer beam was oriented such that the cutting and lateral loading is aligned along the sides of the beam and parallel to their corresponding neutral planes. This design enables the beam to be symmetric in geometry and ensures that the maximum amount of strain will be experienced at the transducer surface when cutting and lateral forces are generated.

A key aspect of the transducer design is the length-to-width ratio. As the ratio decreases, the size of the beam's width increases and/or the beam's length decreases to compensate for the increased amount of shear stress in the beam. This effect makes the shear stress important to measure. To reduce this shear stress to a negligible level, the transducer beam was designed with a greater than 10:1 length to width ratio. This assures that the shear stress is negligible; only bending stress would be measured. This simplified the strain gage circuit required.

The transducer design also employs another design element, the cut-out section. The cut-out section is a slot machined in the center of the transducer, located near the blade holder side of the beam. The cut-out section runs through

the beam in the same direction as the lateral force and aids in measuring the stabbing force by reducing the cross-sectional area of the transducer beam, thereby amplifying the strain measurement.

2.1.2. Measurement System

This system uses several standard techniques from the measurement industry to determine the strain on the surface of a material body using strain gage and strain gage circuitry. The forces are measured through three pairs of strain gages placed on the surface of the transducer: stabbing force (Figure 1-A) and cutting and lateral force (Figure 1-B and C). The first pair, which measures stabbing force, is mounted in the center along the sides of the transducer cut-out, which is on the blade holder side of the transducer beam. The stab strain gages were mounted at this location because the cross-sectional area reduction increased the strain amount created by the applied axial force. The other pairs, measuring cutting and lateral force, are mounted at the fixed end of the transducer beam where each side of the beam received a gage, shown in Figure 4. The cut and lateral strain gages were mounted at the fixed end because the maximum strain amount created by the applied force produces the maximum moment at the fixed end. This is seen in Figure 3. By placing the cut and lateral strain gages at this location, the strain gage would exhibit a high strain signal over any other location on the transducer beam. All strain gages are mounted with the gage length oriented parallel to the length of the transducer beam.

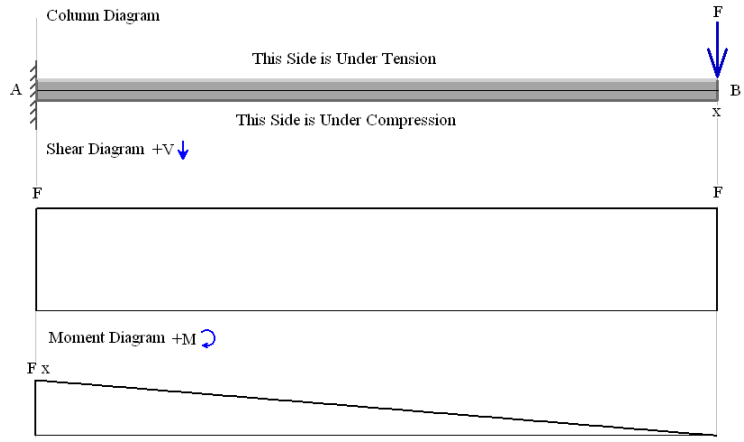

Figure 3: Bending Shear and Moment Diagram.

In this particular device, the strain gages were selected primarily based on size and sensitivity, given the diminutive size of the beam (width of 0.012") and expected force level. Vishay Measurement Group strain gages with 350 ohm resistance, effective gage area of 1/8 x 1/16 inch, and a gage factor of 2.105 were chosen. The strain gages are attached to the surface of the transducer element with strain gage adhesive, M Bond 200 by Vishay Measurement Group. Based on the approach used for designing the transducer beam and measurement system accurate force measurement should be achievable, with a low-level of noise and error in the test system.

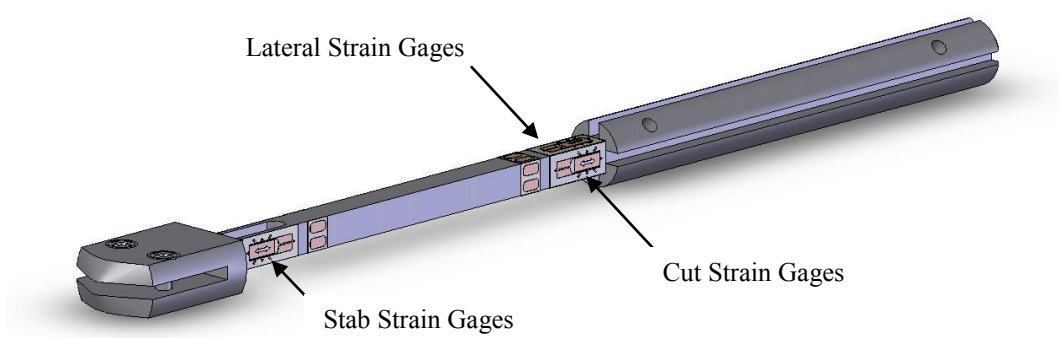

Figure 4: Transducer Apparatus with Labeled Strain Gages.

To measure the desired forces, Wheatstone Bridge strain gage circuits were used. In these circuits, the strain gages act as variable resistors. The resistance in an active strain gage, the gage that is mounted to a surface that deforms during application of force, will change based on the external force applied to the transducer. To determine the stabbing force from the strains, a pair of strain gages was mounted to the transducer apparatus, aligned such that the gages would measure axial compression of the beam. The strain gages were connected to opposite sides in a Full Bridge Wheatstone Bridge circuit, as shown in Figure 5-A and B. As indicated in Figure 5-B, four strain gages are typically utilized in a Wheatstone Bridge. Given that only a pair of active strain gages is used to measure stabbing force in this design, two dummy gages (gages with the same electrical resistance as the active gages, but mounted in a location where no strain is expected) are connected to complete the bridge circuit. To determine the cutting and lateral movement forces, a beam bending approach with two strain gages in a Half Bridge circuit was used (Figure 5-C and D). The transducer wiring contained a pair of strain gages with one of two possible circuit wiring plans based on which force was being measured. In Wheatstone Bridge operation, constant voltage, E, is applied to the circuit and a voltage measurement, e_o, across the middle of the parallel circuit is recorded. The ratio of the voltage over the applied voltage is directly related to sensitivity of the strain gages, the force applied to the system, and the material properties and geometry of the beam where the gages are mounted, as indicated in the equations shown in Figure 5-B and D.

A. Axial column with two gages opposite arms to measure stabbing force.

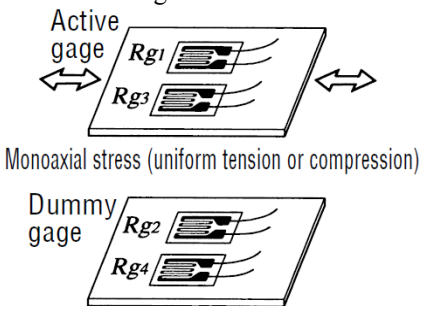

B. Axial column with two gages opposite arms circuitry diagram and strain equations.

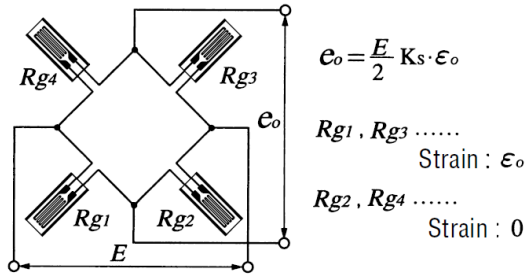

C. Beam bending with two strain gages to measure cutting and lateral movement forces.

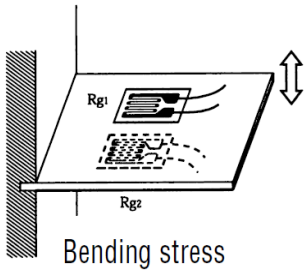

D. Beam bending with two strain gages in a half bridge circuitry diagram and strain equation.

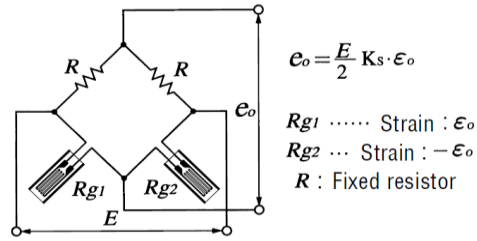

Figure 5: Strain Gage Diagrams, Circuitry, and Equations.

2.2. Test System

The test system, shown in Figure 6, was designed to directly communicate with the Instrumented Handle by relaying instruction commands (e.g. send and receive) and recording the individual force measurements.

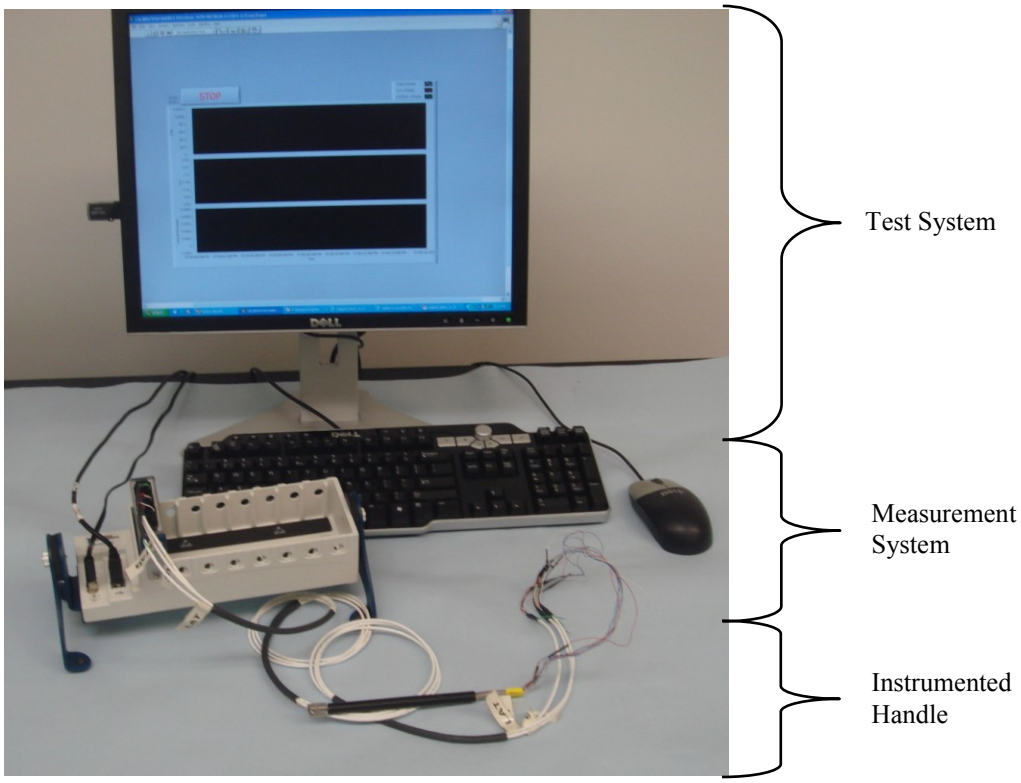

Figure 6: Test System, Measurement System, and Instrumented Handle.

A National Instruments LabVIEW program was developed to control the Instrumented Handle. The program could send and receive commands, start and stop operations, calculate and analyze the force measurements, as well as record live data. The program communicates with the Instrumented Handle through a National Instruments CompactDAQ Data Acquisition system. The CompactDAQ system includes a NI cDAQ-9172 chassis and NI 9219 module, which translates the voltage measurements in the Instrumented Handle to strain measurements in the program.

2.2.1. Software Interface

The LabVIEW based Program, as seen in Figure 7 (user interface) and Figure 8 (LabVIEW code), controls the CompactDAQ Board communications to record the continuous data stream. During testing, the strain data representing the

stabbing, cutting, and lateral directions and loading conditions on the instrument are displayed. The LabVIEW algorithm uses a timed loop to acquire the three streams of strain data via the CompactDAQ hardware at a predetermined rate and save the data in CSV (Comma Separated Value) format.

Figure 7: LabVIEW Program Interface.

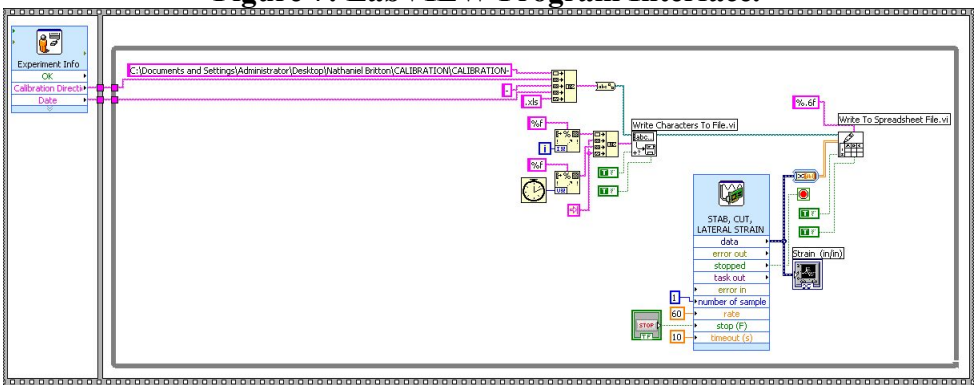

Figure 8: LabVIEW Program Structure.

3. Materials and Methods

This section outlines the material and methods that were used during Instrumented Handle evaluation experiment. The materials consisted of surgical blades (i.e. Becton Dickinson 376500 and 376700 blades), media (Dragon Skin® and porcine loin), and media fixturing and the methods consisted of calibration and post-processing.

3.1. Surgical Blades

After designing the test system, several blades designs were evaluated. The rationale for testing multiple blades concerns applicability. For example, a scalpel blade is designed for the general-purpose cutting of multiple tissues; whereas, a specialized surgical instrument is targeted for specific tissue types (e.g., an ophthalmic blade meant for eye tissues). Therefore, the blades used for testing were selected based on several factors, including size, bevel type (double bevel, single bevel), tip, cutting angle, and the overall geometry, which were expected to have a direct influence on cutting forces. Selecting different blade geometries should show that the instrument is able to differentiate between different applied forces to the blade.

A. BD 376500 Blade

B. BD 376700 Blade

Figure 9: BD's 376500 and 376700, respectively.

The 376500 and 376700 blades manufactured by Becton Dickinson Medical Ophthalmic Systems, shown in Figure 9, were selected for testing. Both of these blades are a double bevel design, which means blade edge bevels are angled on both sides of the blade symmetrically. The blades differ in the angle of cutting edge and blade tip. The 376500, shown in Figure 9-A, has a straight cutting edge but angled towards the blade shaft. The blade tip is formed by the cutting edge bisecting both edges of the blade shaft, creating a very pointy tip. The 376700, shown in Figure 9-B, has a straight cutting edge is that is parallel with the edges of the blade shaft. The blade tip is formed from the cutting edge being rotated 90 degrees, creating an arc shape. These blade geometries should demonstrate that the instrument could differentiate between the applied forces in different blade designs. These blades were originally designed for ophthalmic surgeries, but with the development of new products competing for the same market space, these blades are also being used for cardiovascular and other surgeries.

3.2. Cutting Media

Two materials, Smooth-On's Dragon Skin® and porcine loin, were selected to aid in the evaluation of the Test System and characterize system's capability. These materials were selected to mimic human tissue. Dragon Skin® was selected based on it mold ability and porcine loin was selected to mimic human tissue because it has similarly biomechanical properties to human muscle tissue.

3.2.1. Dragon Skin®

The Dragon Skin® medium is a product that is produced by Smooth-On and is a high performance silicone rubber. Dragon Skin® 10 and MTT Technologies Group 800 Catalyst (Catalyst) were mixed together in a multi-step process. Both materials are in a liquid state before curing in a sample mold. The sample mold creates 8 sample test strips which are 1" by 2" by 1/8" thick.

Dragon Skin® 10 and Catalyst were measured out in a 10:1 ratio, respectively, and mixed in a plastic cup by manual stirring for approximately 5 minutes. Next, the plastic cup was placed into a MCP Vacuum Chamber System and stirred with a mixing blade for 40 minutes or until all visible entrapped bubbles disappeared. This procedure allowed the Dragon Skin® 10 and Catalyst to be uniformly mixed. Then, the mixture was poured into 50 milliliter syringes. A silicone lubricant was sprayed into the sample mold, and then the Dragon Skin/Catalyst mixture was injected into the sample mold cavities. The sample mold was placed into an oven set to125°F. The sample remained in the oven for approximately forty-five minutes. The mold was then removed from the oven and

allowed to cool before the samples were removed from the mold. This process was used to produce rectangular test strips (1” by 2” by 1/8” thick). The test sample thickness varied because the mold was filled from one side and there was limited control of the amount of material injected in each mold cavity. The variability of thickness could possibility influence the measurements, the height of each molded samples was measured prior to each experiment. The thickness ranged from .0929 to .122 inches.

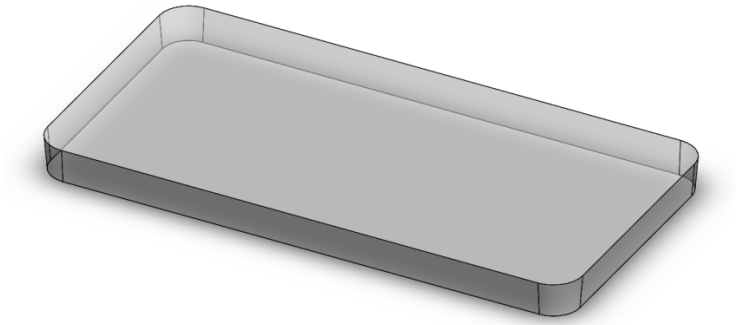

Figure 10: Dragon Skin® Test Sample.

Figure 11: Dragon Skin® Medium Sample Mold.

3.2.2. Porcine Loin

Porcine loin medium was procured from a local grocery store's meat department. The porcine loin medium was kept in a cooler on ice until the sample preparation could be done. The medium was sliced into 2 inches wide by .25 inch thick strips from the roughly center of the porcine loin. Then, these strips were cut into several pieces, resulting in 2" by 2" by .25" thick samples. The samples were prepared in this way so the tissue structure would be similar from sample to sample.

Figure 12: Porcine Loin Test Sample.

3.3. Media Fixture

The two mediums, Dragon Skin® and porcine loin, were placed in a media fixture for testing on an Instron universal testing machine, which was an Instron 3366 Dual Column Tabletop Universal Test with Instron's Bluehill software. The Instron 3366 has a total linear travel of 1122 mm with a speed range of 0.01 to 0.001 millimeters per minute. The load cell used was an Instron 2530-428, with

10 Newton capacity in tension or compression. The load cell served two purposes: 1) to measure and record forces and 2) to interface with the controller to manage linear actuator movements.

The medium and the force direction dictate the design of the media fixture. Since the medium samples were roughly ⅛ inch thick, a clamp fixture with a top and bottom plate was designed to sandwich the medium, shown in Figure 13. The sample medium was placed on the bottom plate, and then the top plate was placed over both the sample and bottom plate. Finally, bolts and nuts tightened the plates together, which removed the slack in the medium for firm positioning during testing. Given the need to orient the medium correctly during tests, an adjustable Instron interface rod (shown as the rod with the single hole in it) could be mounted either perpendicular, Figure 13-A, or parallel, Figure 13-B, to the medium.

A. Stab Fixture B. Cut Fixture

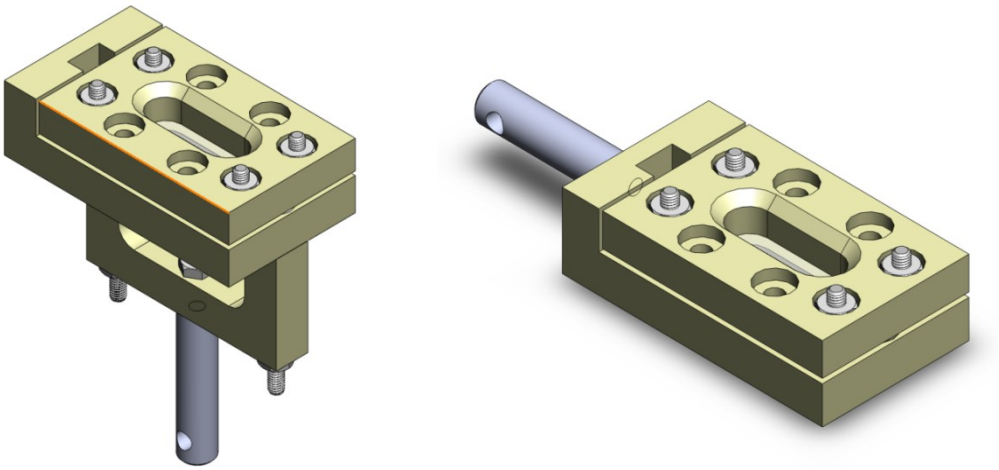

Figure 13: Stab and Cut Fixture, respectively.

3.4. Post Processing Method

The post processing method consisted of three steps: filtration, offset correction, and conversion of the Instrumented Handle data. A National Instruments LabVIEW program, shown in Figure 14 (user interface) and Figure 15 (LabVIEW code), was developed to aid in post processing. During post-processing, the recorded strain data, filtered strain data, converted strain force data and the Instron force data are displayed. The LabVIEW algorithm uses a timed loop to read the recorded Instrumented Handle strain and Instron force data, apply a filter, perform offset correction, convert the data to the appropriate units, as well as save the data in CSV (Comma Separated Value) format.

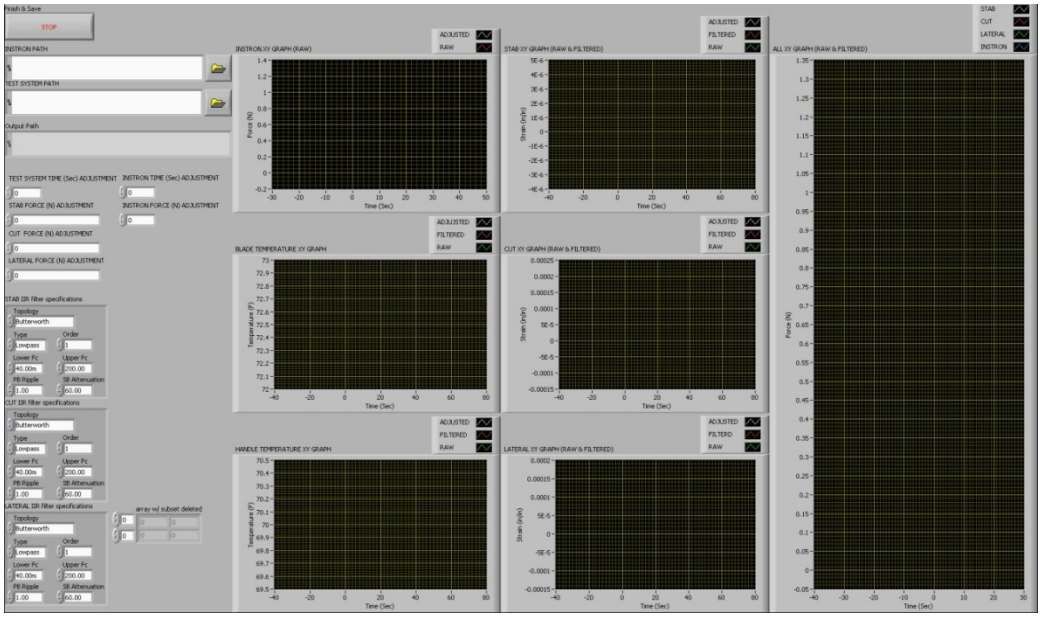

Figure 14: LabVIEW Post Processing Program Interface.

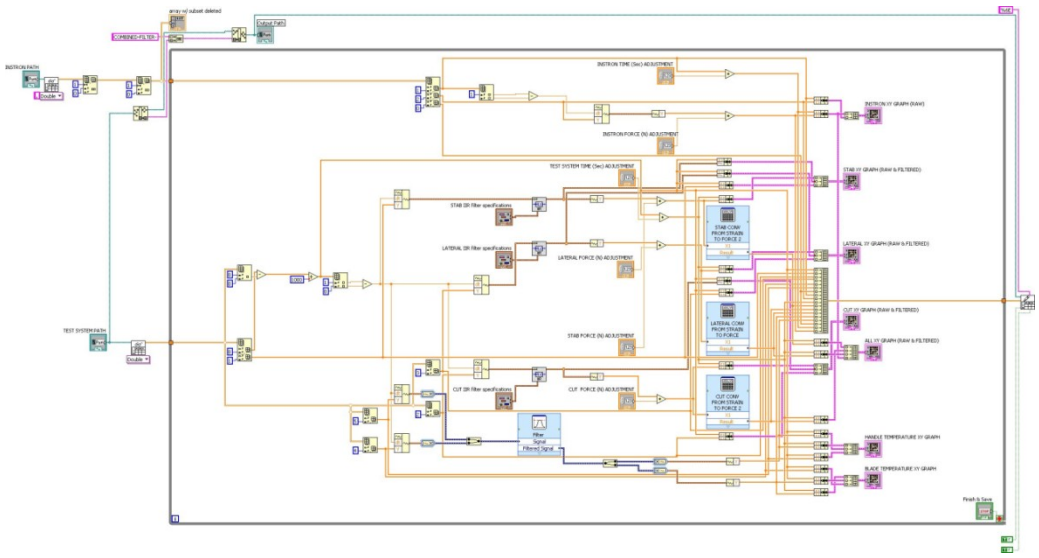

Figure 15: LabVIEW Post Processing Program Structure.

3.5.1 Filtering

The raw strain data measured by the CompactDAQ data acquisition hardware exhibited a high-frequency oscillation. The high-frequency oscillation could be due to electrical noise. Electrical noise could be caused by radio waves, electrical signals in the test room and poorly regulated power received by the Test System and/or an antenna effect generating current in the Test System's wiring. This oscillation masked the stab strain signal somewhat. To remove this oscillation from the stab, cut, and lateral signal, the data was filtered using a Butterworth Low-pass filter. This type of filter works by completely eliminating all frequencies over a cutoff frequency for the stab, cut, and lateral frequency. The cutoff frequency was determined to be 40Hz, 20Hz, and 20Hz, respectively. These cutoff frequencies were selected to remove the oscillations without sacrificing the normal oscillatory behavior expected in the data.

3.4.1. Offset Correction

After the data was filtered, an adjustment was made to synchronize the Test System and Instron profiles using force (strain) measurement offset and a time correction. A tare adjustment is required to compensate for recorded response whenever no force or strain is physically applied. This is accomplished by adding or subtracting a constant to the force or strain measurements. Data acquired in the first 10 seconds of acquisition, before Instron motion began, was used to determine the tare levels necessary. In order to compare measurements from the Test System and Instron results, a second adjustment was needed to synchronize both data acquisition and Instron data measurements in time. This adjustment consisted of adjusting the initial timestamp for both data streams so that when a change in Instron data occurred, the Instrumented Handle data changes would correctly reflect the Instron changes. The time adjustment ensured that the moment before the change in the force or strain measurement caused by an applied load occurs at zero time synchronized with the physical cutting event.

3.4.2. Conversion

The conversion component consisted of passing the Instrumented Handle strain measurements through the calibration equations outlined in section 3.5. This action transforms the strain gage measurements to force measurements. The calibration data were converted to confirm that the Test System force measurements follow the force profiles produced by the Instron. The Test data were converted using a similar process to validate the capability of the Test System of measuring forces.

3.5. Calibration of Test System

Calibration of the Test System was performed before actual cutting experiments were conducted. The stab, cut, and lateral strain gage circuits were calibrated separately. To isolate each strain gage circuit, the Instrumented Handle was mounted in a custom-designed clamp, as seen in Figure 16. In simple terms, the Instron's crosshead was used to move a mounted material relative to the clamped Instrumented Handle, which was fixed to the Instron load frame. The calibrations were run with a blade that had a blunt tip to simulate the location of the applied force during testing. The Instron load cell data would be used to convert the Instrumented Handle strain readings into actual force values. Positioning the clamp in the correct location and orientation would ensure the linear motion of the Instron machine would be aligned with the target measurement axis of the Instrumented Handle, as seen in Figure 16. A linear strain/force profile was achieved during calibration by controlling the Instron's crosshead with constant velocity. Working in this linear range facilitated the development of a calibration equation to convert the stab, cut, and lateral strain to force. The stabbing velocity was set to 0.005 mm/s and the cutting and lateral velocity were set to 0.01 mm/s. These slow velocities were chosen so the force application could be considered static in nature and to increase precision in the calibration.

A. Stab Calibration Setup B. Cut Calibration Setup C. Lateral Calibration Setup

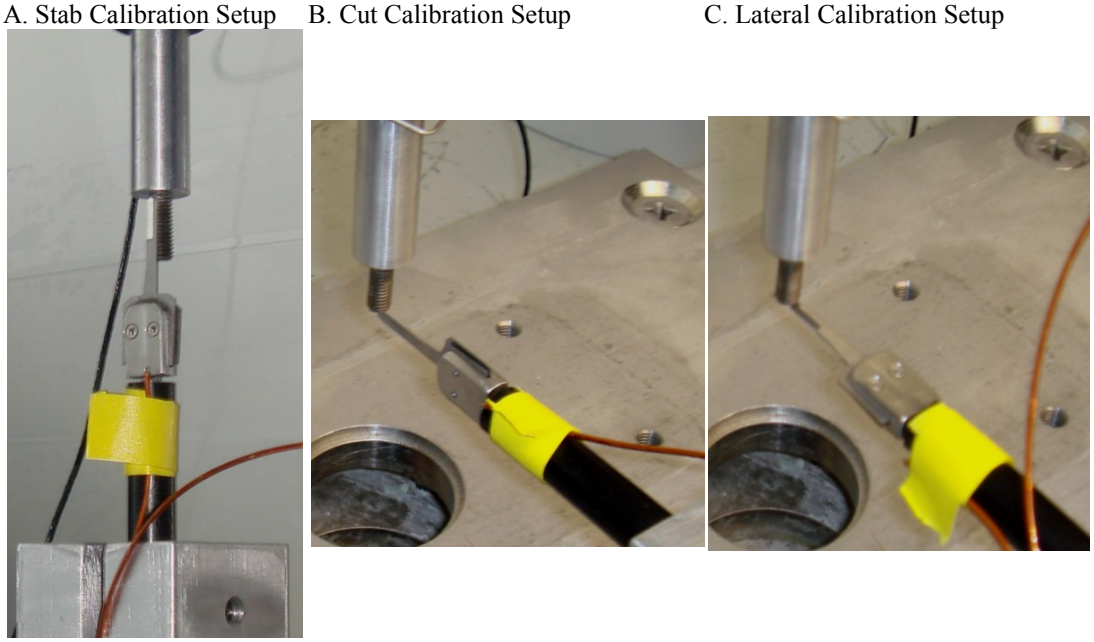

Figure 16: Stab, Cut, and Lateral Caliration Setup.

Calibration equations were developed for stab, cut and lateral strain gage circuit individually. These calibration equations are vital in accurately determining the forces applied to the blades during surgical procedure. To create the calibration equations, post processed Test strain profile data and Instron load cell (force) data on corresponding linear ramp sections were analyzed using a linear regression analysis. The methods for post-processing are discussed in Section 3.4. It was desired that the goodness of fit value (R-square) of the trend line equation from the regression analysis exceed 0.90. The closer the R-square value is to 1 the better the trend line equation matches the data. The calibration equations were constructed using the slope (m) and intercept (b) from the trend line equation according to Equations 2 through 4.

(2)

(3)

(4)

4. Evaluation

Several experiments were conducted to evaluate the Test System and to understand its force measurement capability. The first experiment evaluated the Test System in conjunction with both blades and the Dragon Skin® medium. The second and third experiments investigated the stab strain data drift seen in experiment one. The fourth experiment evaluated the Test System in combination with both blades and Dragon Skin® after the drift correction. The final experiment assessed the Test System in combination with both blades and porcine loin medium. Although the lateral strain gages were calibrated and measured during these experiments, only the cutting and stabbing strain forces were evaluated in these experiments because the cut and the lateral strain gage design were identical.

4.1. Initial Dragon Skin® Cutting Experiment

The first experiment was to evaluate the Test System using the Dragon Skin® medium, with 376500 and 376700 blades, as outlined in section 3.1. This experiment was conducted by isolating the stab and cut strain gage circuit and applying constant velocity for a predetermined travel distance with the Instron 3366 while measuring the strain. The stab and cut operations were conducted separately; the strain gage circuit isolation was conducted by the same method outlined in section 3.5. By ensuring the Instrumented Handle was mounted in this fashion, the Test System would only measure the applied strain in the desired force direction, as shown in Figure 2-A, B, and C. The constant velocity of 30mm per minute was applied to the Instrumented Handle by the Instron for a

predetermined distance of 25mm. This velocity was chosen because a human has the ability with training to replicate this velocity. In this experiment, a stab and cut tests were performed five times with 376500 and 376700 blades each.

4.2. Stab Strain Gage Evaluation Experiments

The Stab data demonstrated a possible drift. It is unclear whether this drift was linear or non-linear or whether the drift occurred in the calibration or testing phases of the experiment. If the drift was linear and had occurred during the calibration test, then the stab Calibration Test System and Instron force profile could match but there could be a mismatch between the Stab Test System and Instron force profile. On the other hand, if the drift was non-linear and occurred only during the stab testing, there would be a mismatch between 1) the stab Calibration Test System and Instron force profiles and 2) stab Test System and Instron force profiles. Then, if the drift was non-linear and occurs during Stab Testing, the Stab Calibration Test System and Instron force profile could match but the stab Test System and Instron force profile would not match. Based on these questions, an experiment was designed and executed to understand where and when the drift was occurring.

After reviewing calibration data and test data from the Initial Dragon Skin® Cutting Experiment, several evaluation experiments were conducted to understand this problem. This mismatch could have been caused by testing outside the range of the Test System or by the influence of temperature fluctuations; therefore, these possibilities were tested. First, calibration was performed, and then a step force profile applied to try to understand if the

difference in the Stab Test System and Instron force profiles could be explained by recording in a different range. In this experiment, the medium and media fixture was replaced with an anvil to ensure a step force profile was going to cover the entire force range of the Test System. The step force profile was created by applying a force to the Instrumented Handle in 0.5 Newton increments up to 5 Newtons every 30 seconds.

Another possible explanation of the drift was ambient temperature. The evaluation experiment was conducted by placing the Instrumented Handle into an oven and performing a heating cycle while collecting Stab strain gage measurements. The heating cycle consisted of 10 minutes with the oven off and the oven door open, 10 minutes with the oven door closed, and 10 minutes with the oven door closed and set to approximately 140°F. At the end of the experiment, the oven door was opened and the oven turned off allowing the Instrumented Handle to cool to room temperature.

4.2.1. Drift Correction

After reviewing the evaluation experiments, it was determined the drift was resulting from the changes in heating and cooling of the testing room. The drift could occur during calibration or actual experiments, and would lead to increases or decreases in apparent strain correlated with temperature variations in the room. Based on this evaluation, three modifications were made to the test Instrument System. The first design modification was to redesign the stab strain gage circuit to be more temperature-insensitive. The modified stab strain gage circuit consisted of replacing the two dummy strain gages with two active strain

gages. The new active strain gages where placed at a ninety degree angle and as close as possible to the original strain gages, as shown in Figure 17. This modification would reduce the temperature drift by reducing the distance between the strain gage in circuits, as well as, actively measuring stab shear strain. By reducing the distance between strain gages, the effect of thermal expansion become similar so that all the strain gage demonstrate the similar thermal expansion strain. Also, using a full bridge configuration with four active gages would ensure the strain gages were in close proximity to each other.

A. Axial column with four strain gages to stabbing force.

B. Axial column with four strain gages circuitry diagram and strain equations.

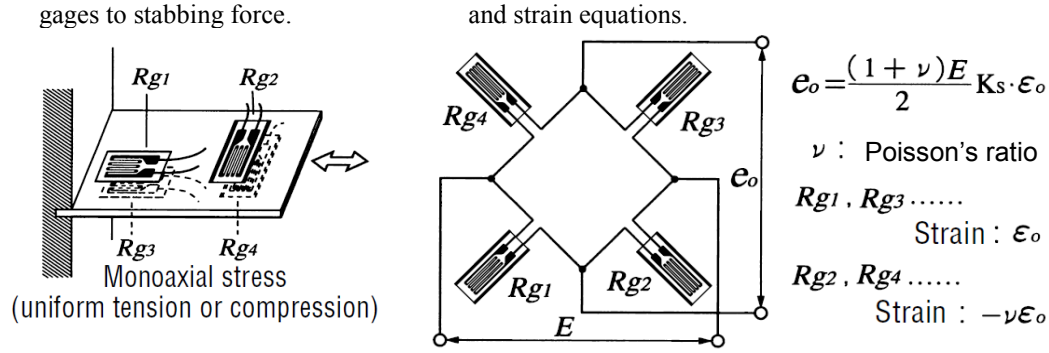

Figure 17: Redesign Stab Strain Gage Circuit.

The active Stab strain gages were Omega Engineering, Inc.'s 175 ohm resistance with an effective gage area of ⅛ inch by 1/16 inch and a gage factor of 2.00. The strain gages were attached to the surface of the transducer element with strain gage adhesive, M Bond 200 by Vishay Measurement Group, as seen in Figure 18.

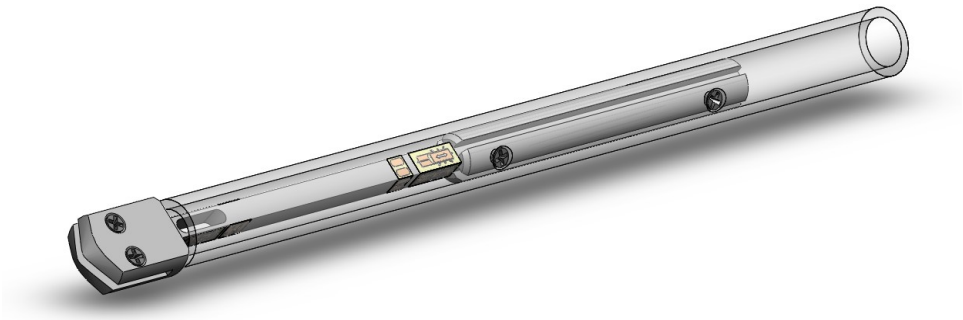

Figure 18: Redesigned Instrumented Handle.

The second modification was to measure temperature. Two thermocouples were added to the Instrumented Handle during the Evaluation Experiment One and Two. These thermocouples were placed near the blade holder, close to the Stab Strain Gage Circuit, and toward the back end of the handle.

The third design modification was to control the environment around the test area of the Instron 3366. A custom chamber encapsulated the Instron testing area and the Instrumented Handle during the Calibration and testing. This chamber was made up of clear plastic sheets which were fastened together and attached to the Instron 3366 with use of Velcro® tabs. The chamber isolated the Instrumented Handle from air movement due to testing room's heating and cooling system.

The changes to the Test System required minor changes to the Program Interface and Program Structure. These changes are seen in Figure 19 through Figure 21.

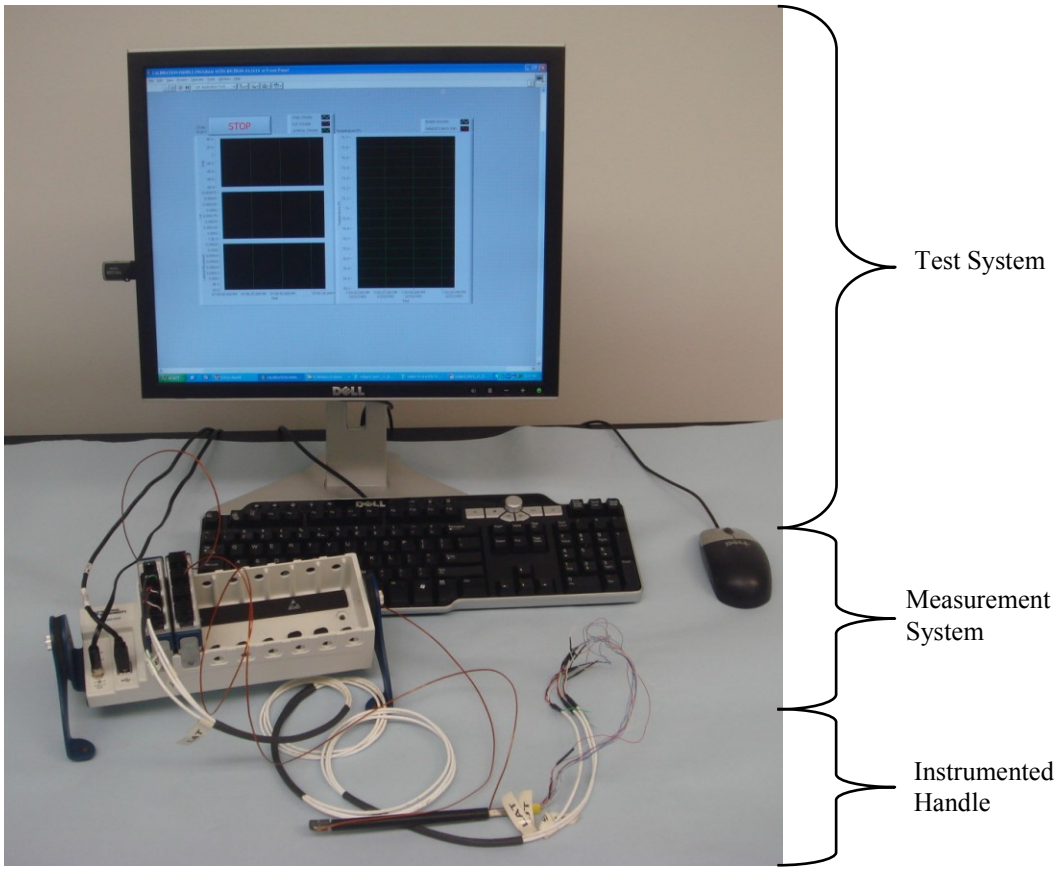

Figure 19: Redesigned Test System, Measurement System, and Instrumented Handle.

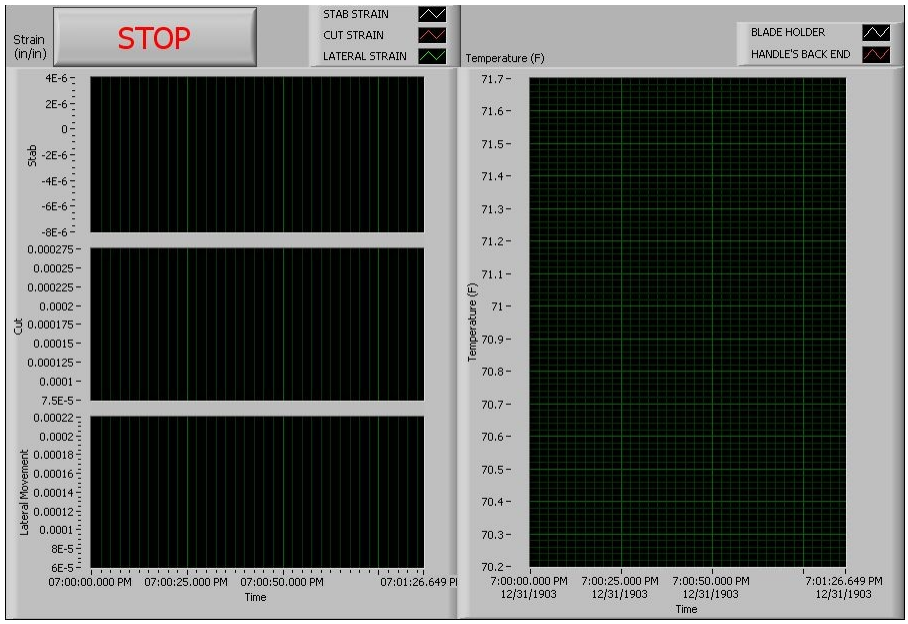

Figure 20: Redesigned LabVIEW Program Interface.

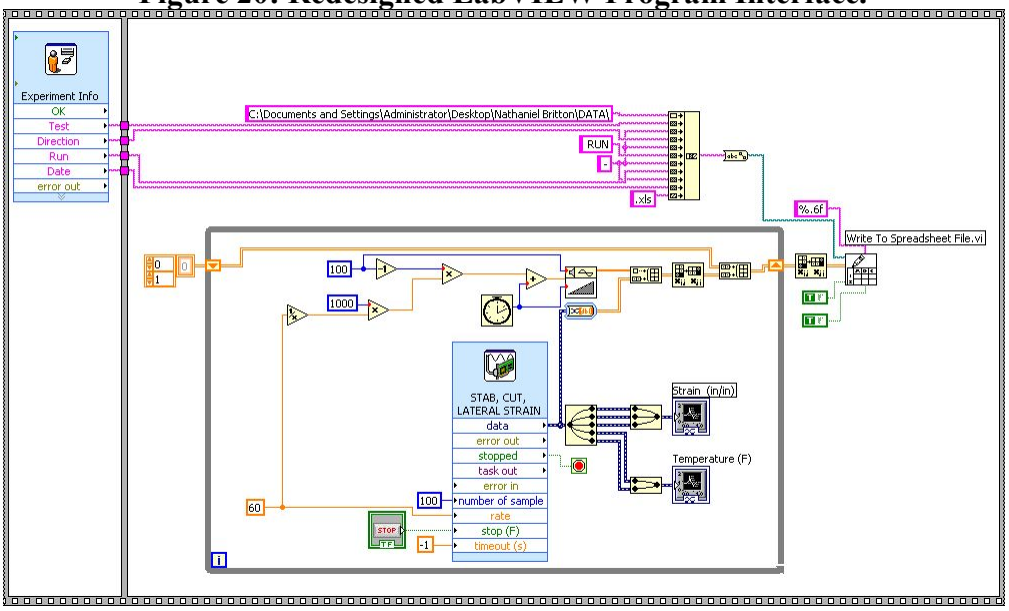

Figure 21: Redesigned LabVIEW Program Structure.

4.3. Damaged Instrumented Handle

After completing the Initial Dragon Skin® Cutting Experiment, the Instrumented Handle was accidentally damaged beyond repair. The transducer beam became bent at the cut-out. Furthermore, the blade holder was not in line with the transducer column and the stab gages came unglued from the transducer

column. It was determined that the Instrumented Handle could not be repaired and had to be remanufactured.

4.4. Dragon Skin® Cutting Experiment

After remanufacturing the Instrumented Handle, the Test System was re-evaluated using the Dragon Skin® Medium as in section 4.1. The same experimental setup and conditions were used to test the Dragon Skin® from the Initial Dragon Skin® Cutting Experiment.

4.5. Porcine Loin Cutting Experiment

The Test System was evaluated using a second material, the Porcine Loin, using the same experimental setup and conditions used to test the Dragon Skin® Medium from Dragon Skin® Cutting Experiment.

5. Results

The section below outlines the results from: atypical calibration, Initial Dragon Skin® Cutting Experiment, Stab Strain Gage Evaluation Experiments, Initial Dragon Skin® Cutting Experiment, Stab Strain Gage Evaluation Experiments, Dragon Skin® Cutting Experiment, and Porcine Loin Cutting Experiment.

5.1. Calibration of Test System

In order to determine the parameters to convert strain to force, the system had to be calibrated. The force from the Instron and strain from the Test System were measured simultaneously. Figure 22 depicts typical time-dependent calibration strain and force profiles for each force: stab, cut, and lateral, respectively.

A. Strain and Force Profile for Stab Calibration

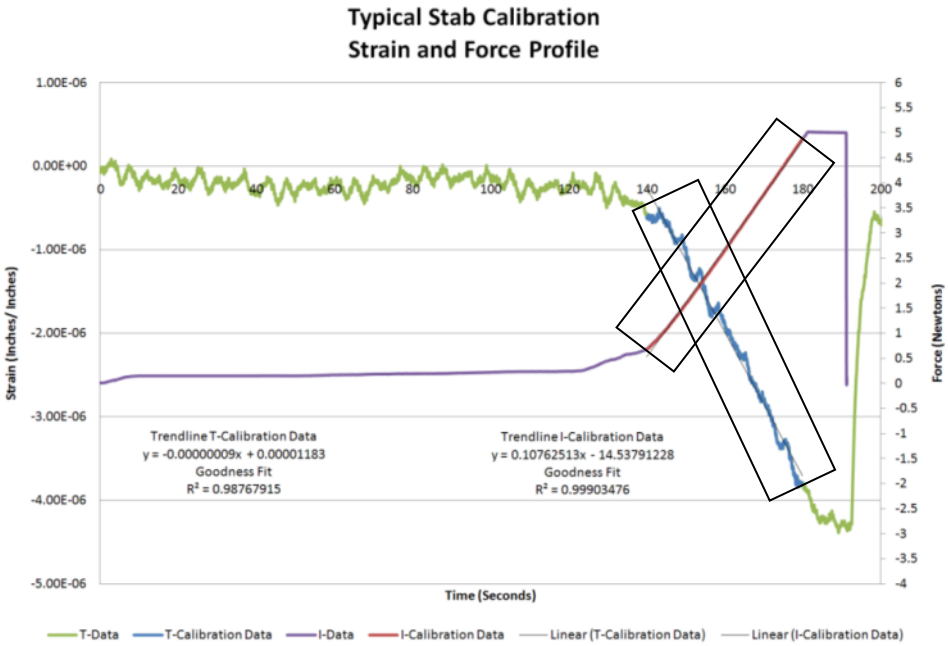

B. Strain and Force Profile for Cut Calibration

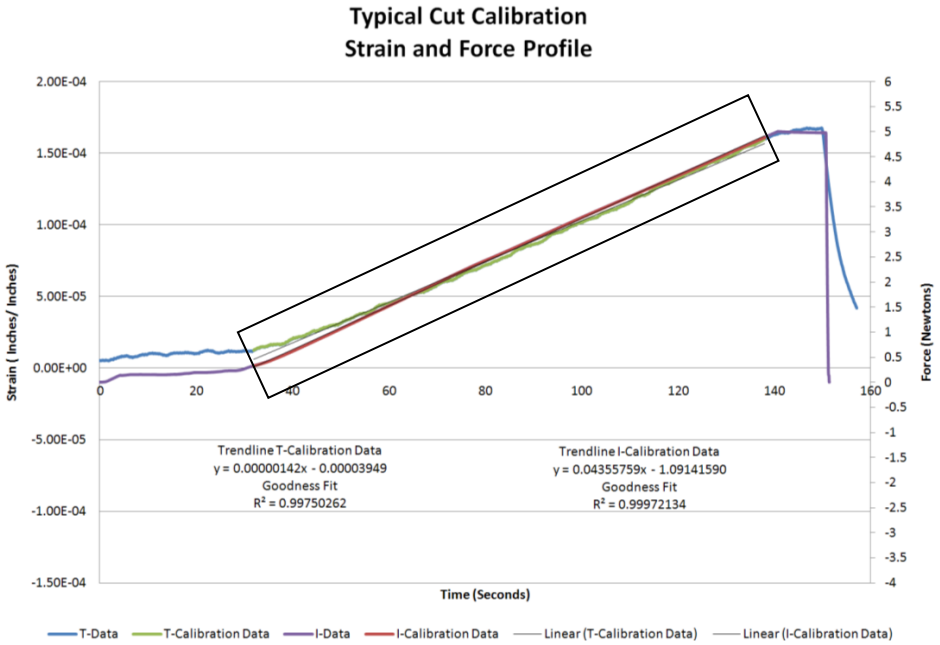

C. Strain and Force Profile for Lateral Calibration

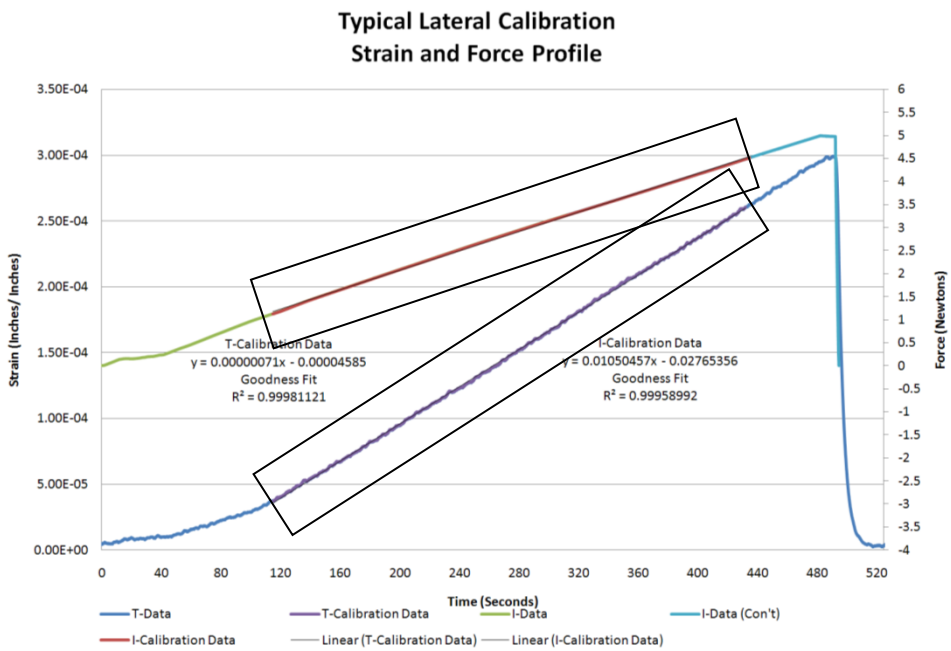

Figure 22: Typical Calibration Strain and Force Profiles.

Figure 22 Legend: The calibration strain and force profiles for A: Stab, B: Cut and C: Lateral forces. The Test System (T-Data) and Instron data (I-data) are graphed. The x-axis represents time with units of seconds and y-axes represent strain with units of inch per inch and Force with units of Newtons. The calibration period is identified by the gray boxes in each graph. Parameters for calibration were identified from the regression lines for T-Data and I-Data during this period. The equations and goodness of fit parameters are displayed.

The calibration data profiles indicate several distinct periods. With respect to force, the first period corresponds to the initial contact of the anvil with the Instrument Handle. This initial contact yielded a force of approximately 0.3N and lasted between 35-135 seconds, depending on the measured force. These initial force levels resulted from the mechanical movement in the calibration fixture caused by the initial loading of the Instrumented Handle. After this initial period, the force ramped to a maximum force of approximately 5N. The ramping time was different for each force because the amount of time required to apply the loads is unique to each cutting operation – 30 seconds for stab, 110 seconds for cut and 440 seconds for lateral forces. During this period, the force and strain

data were linear and served as the calibration period from which the parameters for converting strain to force were identified. The final period of the data collection consisted of a 10 second plateau of measurement. The profile for strain measurements followed similar pattern; however, the force-strain relationship was inversely related in the stab direction. When the force was low, the strain was high.

The calibration period was identified where the data operate in the linear range and the Goodness of Fit of the linear regression was greater than 0.90 (see shaded box in Figure 22). The resulting strain and force equations were derived from the linear regression of this period. All linear regression goodness fit results were greater than 0.9876. From the calibration period, the slope and intercept from the linear regression for strain and force identified in Figure 22 were used to derive the calibration equations outlined in Table 1.

Table 1: Typical Calibration Results.

Direction	(Unit-less, x 10^{-6})	(N, x 10^{-6})	(Unit-less, x 10^{-6})	(Unit-less, x 10^{-6})
Stab	107625.13	-14537991.23	-0.09	11.83
Cut	45355.76	-1091415.90	1.42	-39.49
Lateral	10504.57	-27653.56	0.07	-45.85

Table 2: Typical Conversion Calibration Results	
Direction	Conversion Calibration Equation _____
Stab	_____
Cut	_____
Lateral	_____

5.2. Initial Dragon Skin® Cutting Experiment

In this experiment, measurements of stab and cutting force were made for two blades (376500 and 376700) cutting through a Dragon Skin® medium. The results from 5 samples of testing data are depicted in Figure 23 through Figure 26. Note that while all forces were measured, only the force profiles acting in the applied direction are displayed. For example, if the applied direction was the stab direction, only the stab force profile is shown.

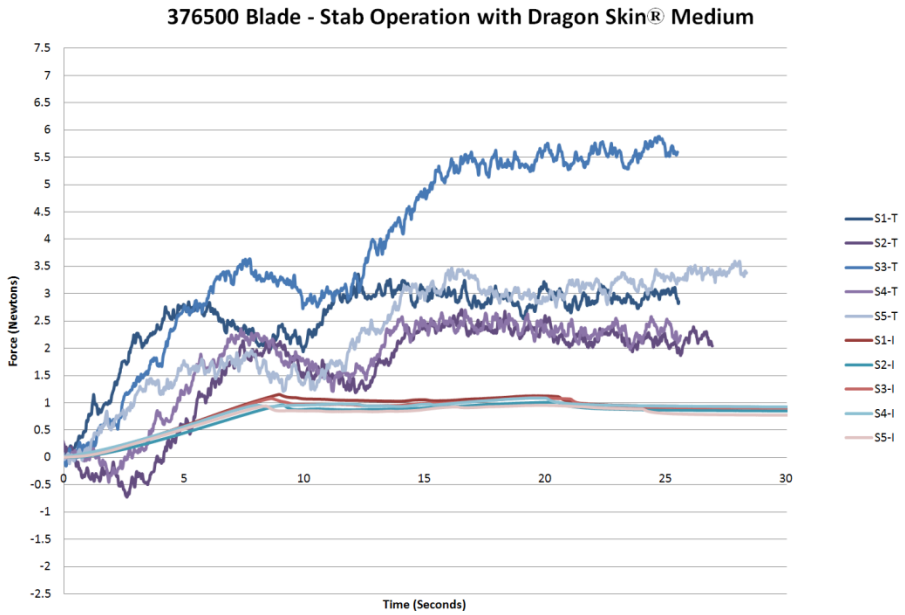

Figure 23: Initial Dragon Skin® Cutting Experiment, 376500 Stab Force Profile.

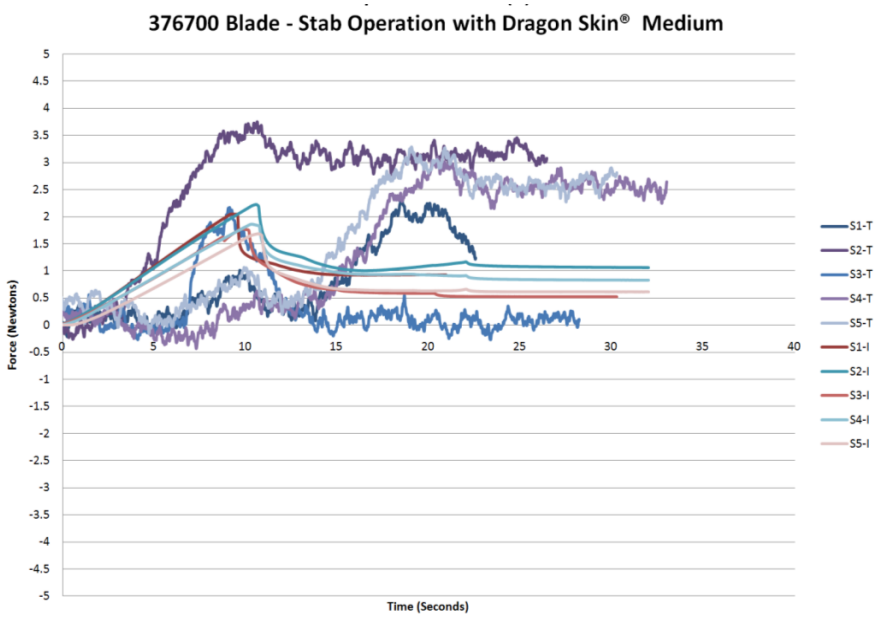

Figure 24: Initial Dragon Skin® Cutting Experiment, 376700 Stab Force Profile.

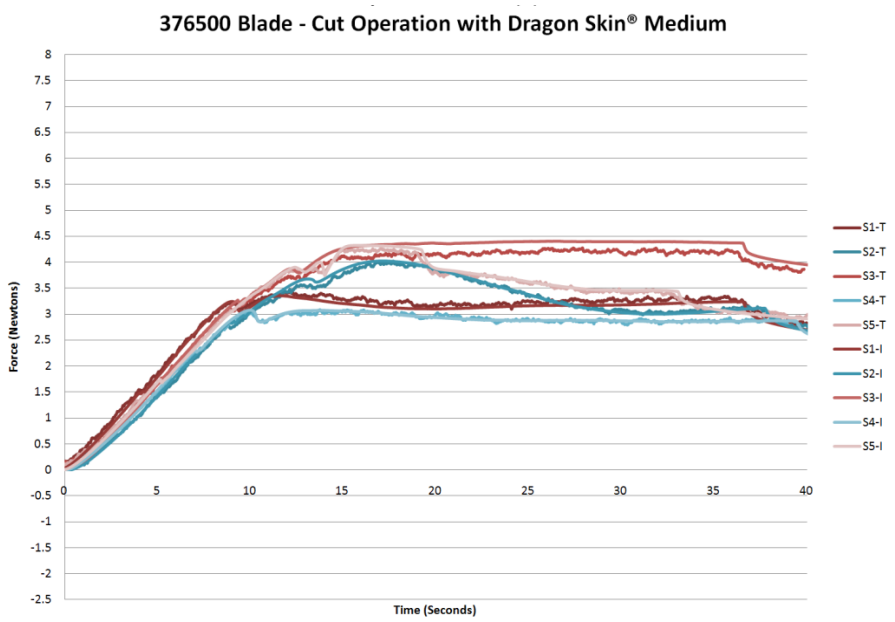

Figure 25: Initial Dragon Skin® Cutting Experiment, 376500 Cut Force Profile.

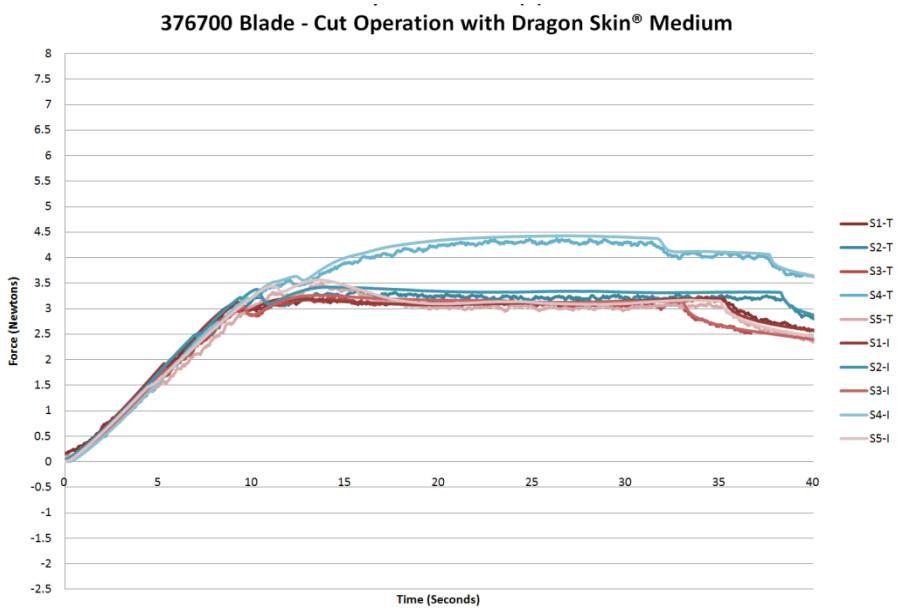

Figure 26: Initial Dragon Skin® Cutting Experiment, 376700 Cut Force Profile.

Figure 23 and Figure 26 Legend: Results of five (5) testing samples (S-#) and from both Test System (T) and Instron (I). The x-axis is time with units of seconds and y-axis is force with units of Newtons.

The data profiles from the test instrument and the standard system followed similar patterns in both the stab and cut directions. Like the calibration curves,

the force profiles had several distinct phases or periods. The first period corresponded to the initial contact of the blade to the Dragon Skin® medium. The stab force steadily ramped to approximately 1N for 376500 blade and approximately 1.75N for 376700 blade. The second period started with a dip in force when the blade made an initial break in the medium and the resulting relaxation of medium from after initial contact. In the final period, the force reached a plateau, corresponding to the blade passing through the medium. This final period yielded force measurements that were roughly 1N for 376500 blade and roughly .75N for 376700 blade. Overall, the force profiles for the two blades had similar patterns.

Likewise, a similar pattern was observed for the cut data profiles. The initial period showed a steady increase in force to approximately 3N for both the 376500 and 376700 blades. The final period yielded a dip in force when the blade made its initial break in the medium. Then, the force profiles increased briefly before reaching a plateau.

5.3. Stab Strain Gage Evaluation Experiments

After observing the drift in the stab direction, several evaluation experiments were tested to determine the cause of the drift.

5.3.1. Initial Drift Evaluation Experiment

In the first experiment, an anvil replaced the blade and three consecutive sample measurements were collected. Figure 27 illustrates the stab step force profiles from this experiment. A series of steps in time and force were created in the force profiles by applying an incremental force to the Instrumented Handle in

.5N increments up to 5N. Each step in force was held for 30 seconds before the next load change.

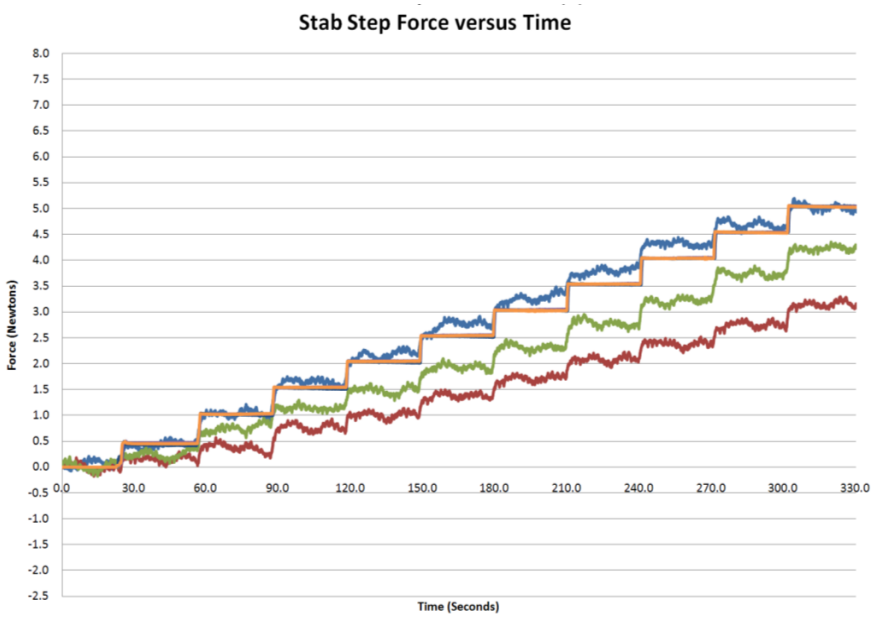

Figure 27: Initial Drift Evaluation Experiment, Stab Step Force Profile.
Figure 27 Legend: The x-axis is time with units of seconds and y-axis is force with units of Newtons.
Blue Profile – 1st Run Test System Force Measurements
Navy Blue Profile – 1st Run Instron Force Measurements
Green Profile – 2nd Run – Test System Force Measurements
Purple Profile – 2nd Run – Instron Force Measurements
Red Profile – 3rd Run – Test System Force Measurements
Orange Profile – 3rd Run – Instron Force Measurements

The force profiles were consistent with the incremental step changes applied to the system; however, the final force level varied between the three consecutive runs. The first sample ended at the 5N; however, the other samples ended at 4.25N and 2.4N. This difference indicated a roughly 85% and 52% reduction in force in the second and third run, respectively, and indicates the Stab Test System force profile appears to decrease over time. The first run and Instron force profile closely matched. This first run was conducted immediately after

calibration; therefore, no drifting occurred between the time of calibration and first test run.

5.3.2. Drift Evaluation Experiment

In the second experiment, temperature was investigated as a possible explanation of the drift seen in the stab data. Temperature was varied and measurements were collected. Figure 28 shows the strain and temperature profile.

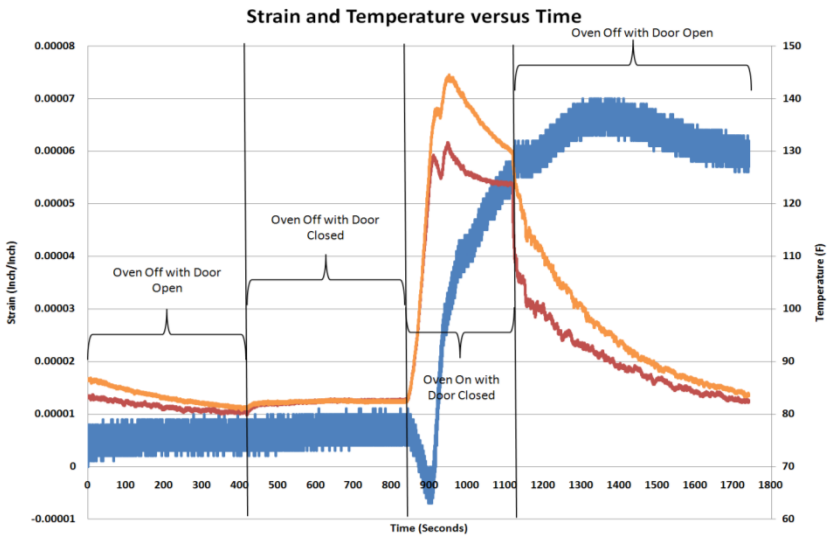

Figure 28: Drift Evaluation Experiment, Strain, and Temperature Profile.

Figure 28 Legend: The x-axis is time with units of seconds and y-axis is strain with units of inch per inch.
Blue Profile - Strain Measurement.
Red Profile - Temperature Measurement from Thermocouple at the Blade Holder.
Orange Profile - Temperature Measurement from Thermocouple at the End of the Handle.

The strain and temperature profiles as seen in Figure 28 illustrated several periods corresponding to temperature changes. The first period was conducted with the Instrumented Handle in the oven with the oven off and oven door open. As the temperature of both thermocouples gradually decreased to roughly 80°F, the strain increased slightly. When the oven door was closed, the temperature increased to roughly 83°F and strain increased until the 700 second mark, where it

began to level out. During this period, the Instrumented Handle was isolated from environmental effects and the strain and temperature measurements were fairly stable over roughly 400 seconds. When the oven was turned on, the temperature increased to over 120°F and the strain decreased for 50 seconds then, before quickly increasing to 0.000066. Finally, the system was returned to the initial conditions of 80°F. As the temperature rapidly dropped, the stab strain measurement gradually decreased.

5.4. Dragon Skin® Cutting Experiment

After redesigning the Instrumented Handle and making modifications to account for the drift caused by temperature fluctuations, the Initial Dragon Skin® Cutting Experiment was conducted again. The force profiles were used to determine if the modifications (three modifications: redesign stab strain gage circuit, thermocouple addition, and environmental enclosure) had reduced the effect of temperature and the drift in the stab data.

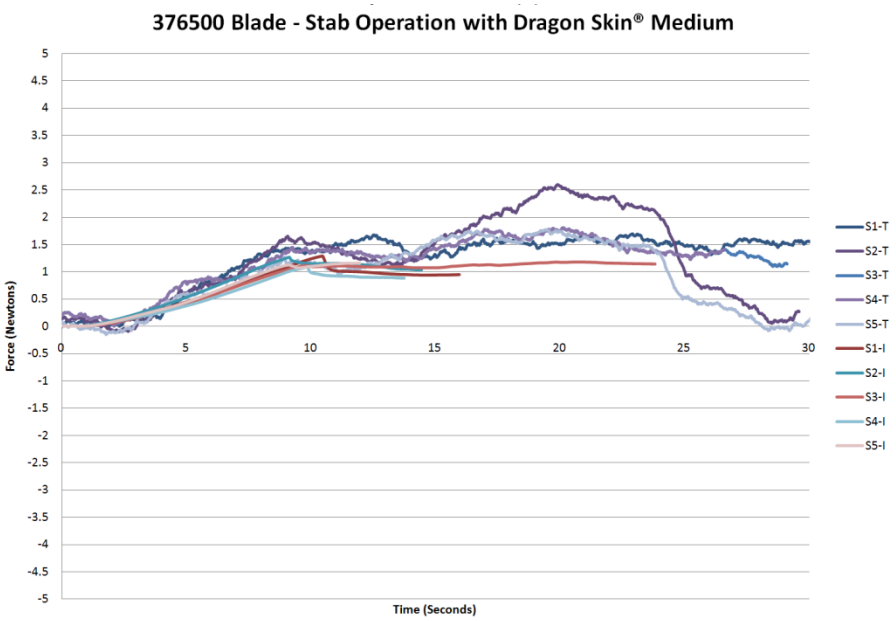

Figure 29: Dragon Skin® Cutting Experiment, 376500 Stab Force Profile.

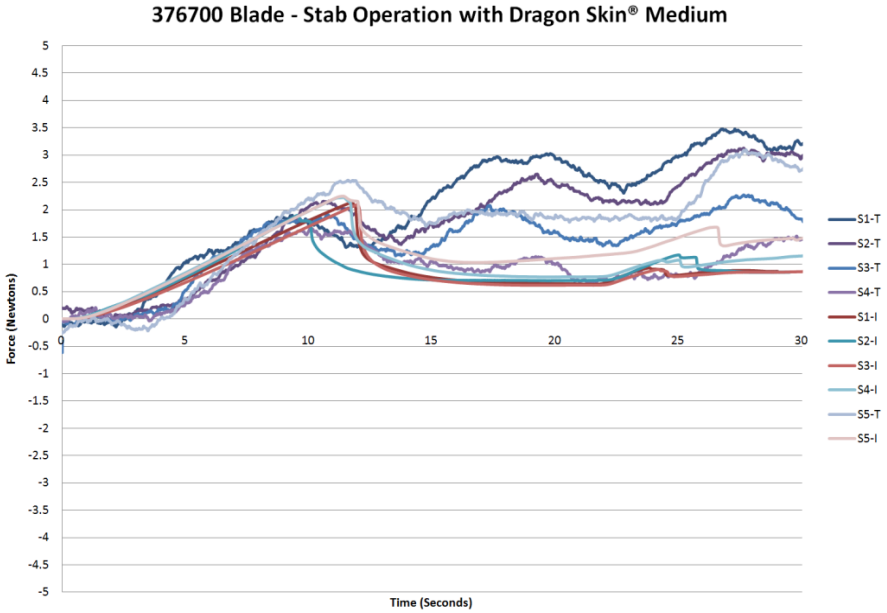

Figure 30: Dragon Skin® Cutting Experiment, 376700 Stab Force Profile.

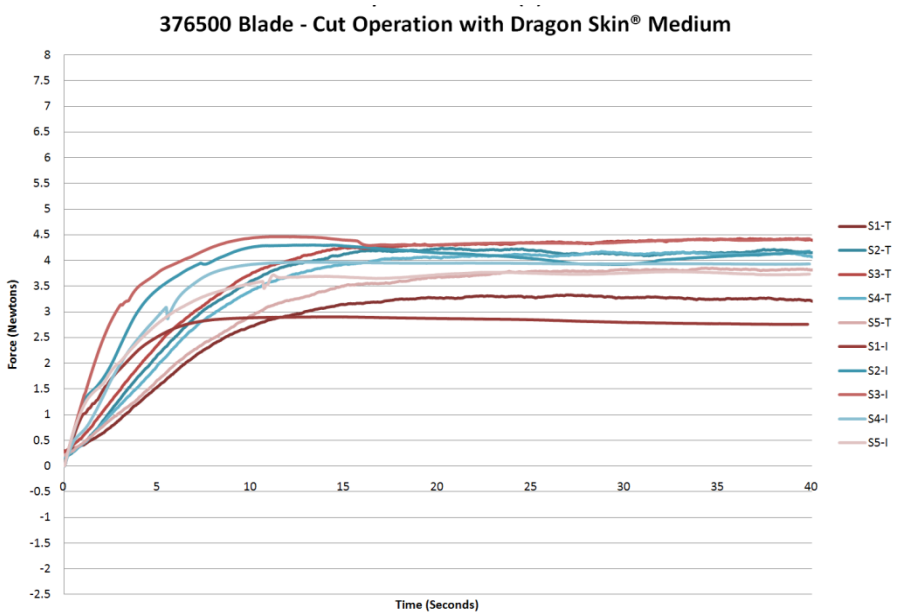

Figure 31: Dragon Skin® Cutting Experiment, 376500 Cut Force Profile.

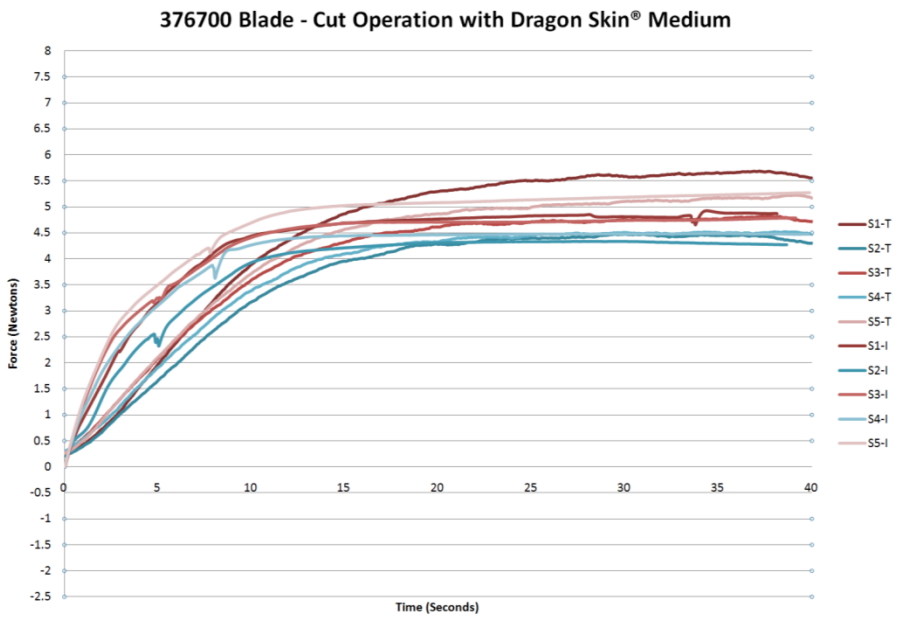

Figure 32: Dragon Skin® Cutting Experiment, 376700 Cut Force Profile.

Figure 29 through Figure 32 Legend: Results of five (5) testing samples (S-#) and from both Test System (T) and Instron (I). The x-axis is time with units of seconds and y-axis is force with units of Newtons.

The stab profiles as seen in Figure 29 and Figure 30 were similar to the profiles seen in Figure 23 and Figure 26; however, the drift was no longer present. In addition, the initial and final forces were different. The initial period yielded a

force of approximately 1.25N for 376500 blades and approximately 2N for 376700 blades. The final period yielded a force roughly1N for 376500 blades and approximately .75n for .376700 blades. During the final period, the test samples deviated from the Instron data, showing a random rise and fall in the measurement.

The modifications to the test system did not affect the cut profiles. As shown in Figure 30 and Figure 31, the test and standard system data are well-matched and show similar patterns as the previous data.

5.5. Porcine Loin Cutting Experiment

In this experiment, the stab, and cut operations were conducted separately on two blades (376500 and 376700) and were tested using Porcine Loin medium using similar methods (see Figure 33 through Figure 36).

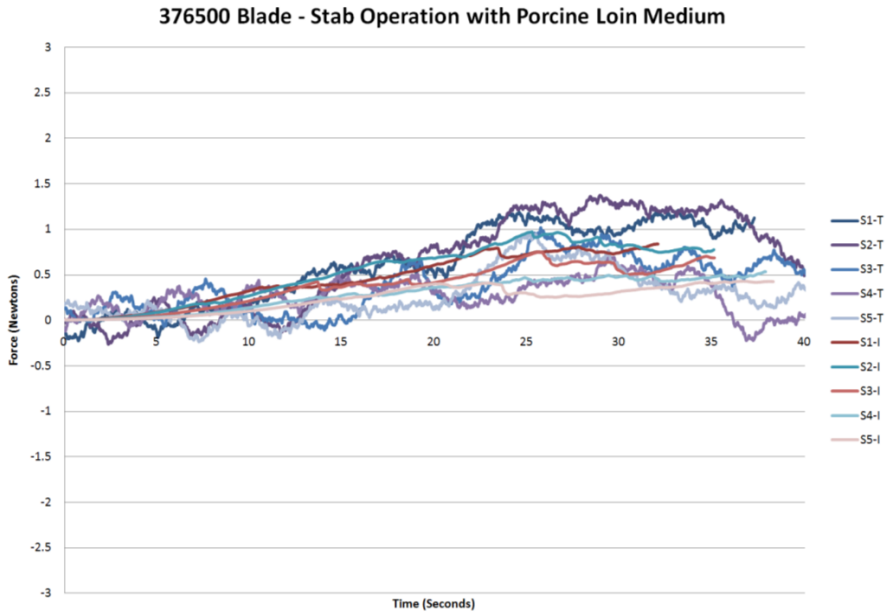

Figure 33: Porcine Loin Cutting Experiment, 376500 Stab Force Profile.

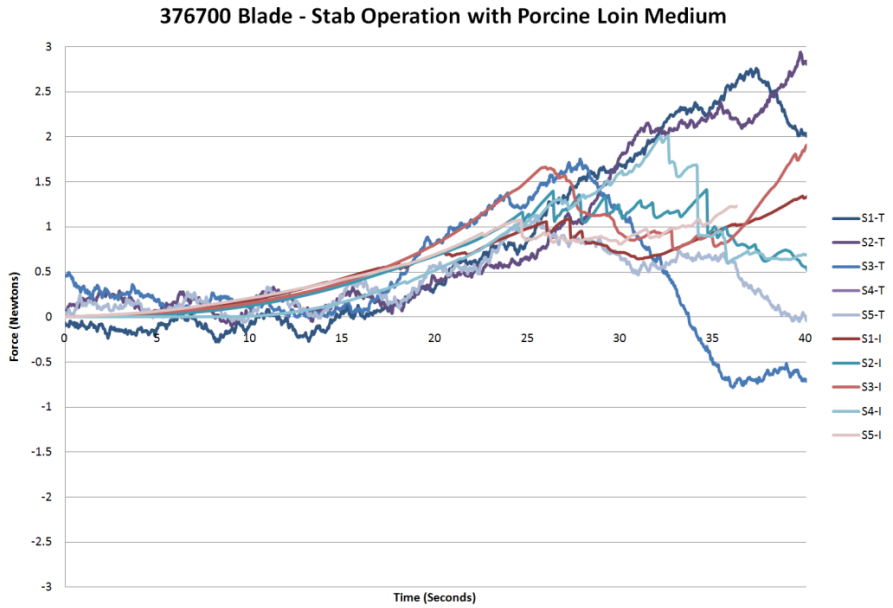

Figure 34: Porcine Loin Cutting Experiment, 376700 Stab Force Profile.

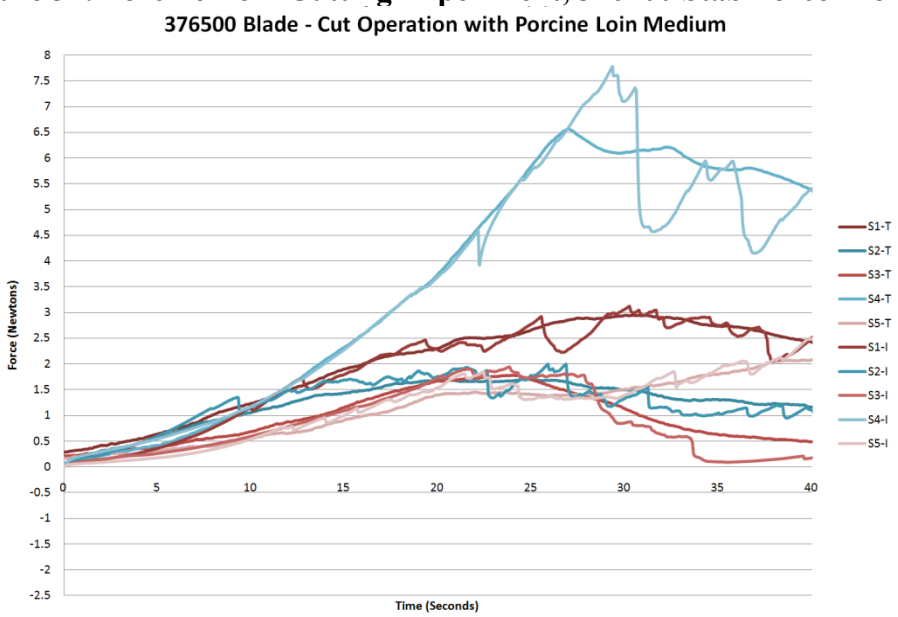

Figure 35: Porcine Loin Cutting Experiment, 376500 Cut Force Profile.

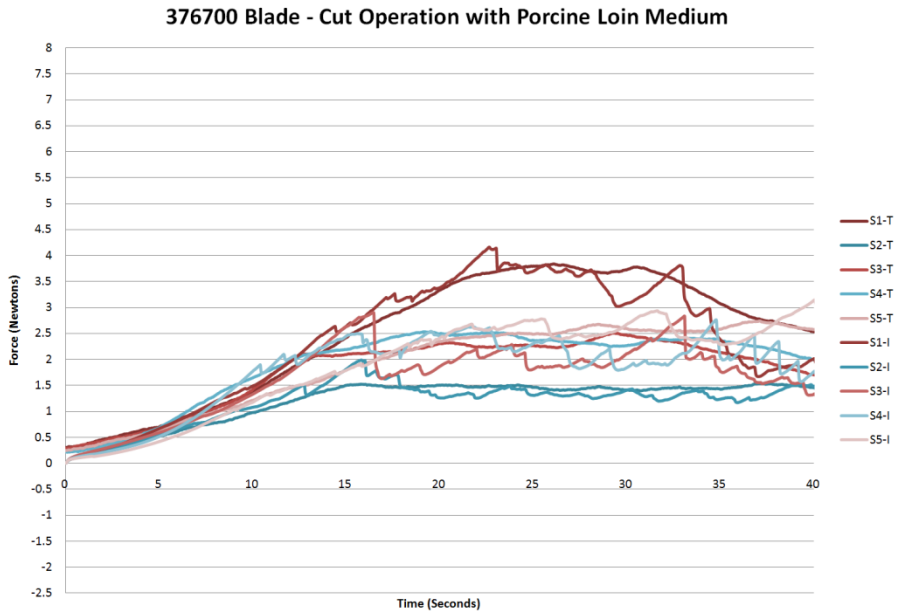

Figure 36: Porcine Loin Cutting Experiment, 376700 Cut Force Profile.
Figure 33 and Figure 36 Legend: Results of five (5) testing samples (S-#) and from both Test System (T) and Instron (I). The x-axis is time with units of seconds and y-axis is force with units of Newtons.

Overall, the data from the test and standard system were similar. The stab profiles, shown in Figure 33 and Figure 34, had two distinct phase or periods. The first period corresponded to the initial contact of the blade to the porcine loin medium. The force steadily increased during this period. The second period resulted in a drop followed by a gradual increase in force, resulting from the initial break in the medium. Surprisingly, during this period using the 376700 blade, all five samples showed different force profile patterns. The force of the first two samples continued rising but unexpectedly, the force of the remaining samples decreased to an unexplained negative force.

The cut force profiles also had several distinct periods. Like the stab force, the first period corresponded to the initial contact of the blade to the porcine loin medium where the force steadily increased. During the second period, the force

measured by the Instrumented Handle was smooth and curvilinear. However, even though the force measured from the Instron followed the same general pattern, the data randomly had risen and fallen around this curvilinear pattern. Unlike the stab data, the point in which the break begins and propagates was not able to be determined. however, in sample four for the 376500 blade, this point of propagation was determined to be approximately 7.75N. This point is defined when the force drops and then continues to rise and fall, which is similar to other cut samples.

6. Discussion/Conclusions

Using a transducer, a Test System was designed to interact with a custom designed Instrument Handle to measure several forces on a blade during surgical cutting operation. To determine the viability of this system, accuracy and reproducibility of the force measurements were assessed. Through experimentation and evaluation, these measurements were conducted in several conditions involving two blades and two different types of medium.

The first objective of this project was to design a system that would reliably and accurately measure the forces exerted on a blade when cutting material. To assess this, the Test System profiles were compared and evaluated against Instron System profiles. The comparison and evaluation were conducted by plotting the data and visually determining trends and visually matching the Test System and Instron System profiles. As the Test System and Instron data matches, the accuracy level increases. All force profiles demonstrated a gradual increase in load over time, which was created by the blades applying load to the surface of the medium. After the gradual increase in load, there was a sudden drop in force profile. The sudden drop was caused by the blade having applied enough force to the medium surface to produce a crack and the medium relaxation at the moment after the blade punctured the medium.

Although the pattern between the test and standard system were similar, visual inspection of the calibration profiles showed that the strain measurements in the test system were noisier than force data in the Instron. This noise level difference could be explained by electrical, mechanical, and/or environmental

effects. With respect to electrical effects, high frequency oscillations in the data exhibited rapid increases and decreases over a short period of time (i.e., milliseconds). Electrical noise could be caused by radio waves, electrical signals in the test room and poorly regulated power received by the Test System and/or an antenna effect generating current in the Test System's wiring. With respect to mechanical effects, low frequency oscillations in the data increases and decreases over an intermediate period of time (i.e., seconds). Mechanical noise could also be caused by vibrations of moving motors and actuators, such as in the Instron System, or in the heating and cooling system, or in the flooring of the building in which test room is located. With respect to environmental effects, data could gradually increase or decrease over a longer period of time (i.e., minutes) and sometimes have a cyclical pattern. For example, heating and cooling systems in the testing room in which the cycle on and off depending on the room's temperature. The effects of temperature were minimized by making modifications to the test instrument. Based on the understanding of where possible noise could come from and how it could influence the measurement, it is likely reasonable to say that the strain measurement noise is a consequence of electrical interference; however, it is difficult to identify the exact source without further testing.

On further inspection, the stab strain measurement demonstrated a higher level of noise over the cut/lateral strain measurements. In particular, as seen in the Initial Dragon Skin® Cutting Experiment before modifications were made, the stab force was particularly sensitive to temperature fluctuations in the test

room. The temperature sensitivity may have resulted through the effects of thermal expansion of the Instrument Handle, although the original design selected a stab strain gage circuit that should have compensated for thermal expansion. The original design should have had temperature compensation, which was made by mounting the dummy strain gages in a location and use of the same material type on the Instrumented Handle close to the active, but in a location where it would not see the strain that the active would applied from stab, cut, or lateral force. Therefore, thermal expansion would have the same effect on both the active and dummy strain gages, theoretically cancelling out the effect. After determining that temperature did affect the system measurement, several improvements were made to the Instrument Handle testing environment. These improvements included changing the stab strain gage circuit to a full bridge configuration with four active gages, adding two thermocouples (one mounted near the blade holder and one mounted at end on the handle), and enclosing the Instrument Handle during calibration and testing.

This noise level difference between stab and cut/lateral may have been caused by the increased sensitivity of the stab strain gage circuit over the cut/ lateral strain gage circuit. This sensitivity difference is based on the chosen type of strain gage circuit for stab, cut and lateral. A full bridge was selected for the stab strain gage circuits and a half bridge circuitry was selected for the cut and lateral forces. The resulting noise level generated by these circuitry selections would be inversely related, where a higher level of noise would be present in the stab force compared to the cut/ lateral forces. Another source of the increased

noise level in the stab direction could be the increased wiring in the stab strain gage circuit over the cut and lateral strain gage circuit. These differences in wiring between the strain gage circuits could be causing the increased level on noise in the stab strain gage circuit. Furthermore, this noise level difference in between stab and cut/lateral maybe a compliance issue in the stab step fixture. Based on the low force levels, the any mechanical movement in the fixture that may occur could translate and create noisy data.

When comparing the force profiles for the two blades (376500 and 376700), there are some noticeable similarities and differences. The 376500 and 376700 blades exhibit an overall similar force profile shape in stab and cut. All the force profiles demonstrated a gradual increase in load over time which was created by the blades applied load to the surface of the medium. This increase in force was caused when the blade had applied enough force to the medium surface to produce a crack. After the gradual increase in load, there was a leveling of load. The leveling was caused by the blade applying enough force to continue the crack propagation and cut the medium. However, the Test System is able to measure the slight changes in force caused by the shape of the blade. The major difference between the 376500 and 376700 blades was the maximum force value measured. The stab force exerted on 376500 blades was smaller than the 376700 blades by about .75N using the Dragon Skin® medium and roughly .50N using the porcine medium. This difference may be associated with the blade's tip design. The 376500 blade tip was designed with a sharp, acute angle with two bevels and the 376700 blades was designed with a larger radial tip with two

bevels creating a small pointed tip, as seen in Figure 9. This tip design allows the 376500 blade to apply more force to one point than the 376700, which applies the force over a larger area, resulting in higher contact stress with the 376500 blade. These design differences create a difference in the way the blade's tip initiated a crack in the medium surface to allow the blade to pass through the medium. In addition, each blade showed a difference in the initial period of the force profile. Both the stab and cut force exerted on the 376500 blade increased at a slower rate than the 376700 force profiles indicated. Again, the blade's tip design may explain this finding in the stab force and the cutting length and angle of cutting edge may explain this finding in the cut force. Compared to the 376700 blade, the 376500 blade requires less force to initiate the crack, and therefore likely requires less time.

Another difference was between the Test System and Instron data. This difference was noticeable after the gradual increase of load. In this section, the Instron force profile showed several sudden decreases and increases of force. owever, at the same time the Test System force profile demonstrated no sudden decrease or increases of force, as seen in Figure 35 and Figure 36. This difference may possibly have been caused by the filtration method used. If a data set is aggressively filtered, the data set would exhibit a less smooth profile, eliminating measurement of actual force fluctuations applied to the blade. In this case, the aggressive of the filter depends on the selected cut-off frequency used in Butterworth Low-Pass.

Overall, this data suggests that force measurements can be made in the stab and cut directions and the Instrumented Handle can be successfully used with various blades and cutting media.

6.1. Future Work

The future work was broken into two areas, which are design improvements and design enhancement.

6.1.1. Design Improvement

Based on the results, the stab transducer, post-process techniques, and Instrumented Handle fabrication may benefit from improvements. The stab transducer improvements would focus on increasing the signal and reducing noise in the stab strain measurement. This measurement is the signal output of the stab strain gage before the post-processing. For future developments, a method of analyzing the signal-to-noise ratio (SNR), described in equation 5, would be created. Understanding the SNR would aid in improving the Stab measurement's sensitivity, accuracy, and repeatability, which is important in the design of a Test System.

$$\frac{\quad}{\quad} \tag{5}$$

Another improvement would be to integrate the post-processing in the LabVIEW Program, as seen in Figure 21, and enhance the filtering technique. Integrating the Post-Processing into the Program would produce filtered, synchronized and converted profiles in real-time. Also, by improving the filtration technique the force profile would better represent the actual forces and increase the accuracy of the force measurements. This idea stems from data

illustrated in the Dragon Skin® Cutting Experiment and Porcine Loin Cutting Experiment figures, where the forces from the Test Instrument did not show the desired agreement with the Instron. In the filtration section, sometimes the force profile appears to be filtered too aggressively and other times the force profile appears to be under filtered. Therefore, improving the post-processing method is necessary to improve the accuracy of force measurements produced by the Test System.

The Instrumented Handle fabrication improvement would focus on the manufacturing of the transducer beam and the strain gage assembly, as seen in Figure 2. This would focus on ensuring the surfaces of the transducer are parallel or perpendicular to each other and the strain gages are aligned properly with the transducer. Making these improvements would ensure each Instrumented Handle could measure strain accurately and reliably.

6.1.2. Design Enhancements

Before implementing the Test System in an *in-vivo* environment, several enhancements would have to be designed and evaluated: additional measurements, implementing on-board electronics for tetherless operation, and allowing for *in vivo* testing.

An enhancement to the Instrumented Handle would be to include other measurement capabilities (i.e., accelerometer and inclinometer). Adding an accelerometer and inclinometer would aid in understanding the distance traveled, speed of travel, acceleration of travel, and angle of cutting action related to the force produced during a cutting action. These variables along with the force

measurements are important for improving simulation-based training systems. Including these measurements into the design of the Instrumented Handle creates another potential area of use for this tool.

Another design enhancement is to make the Instrumented Handle wireless. In the current system, the Test system is tethered to a computer interfaced CompactDAQ data acquisition device. By designing the Instrumented Handle to be wireless enables the surgeon to have unrestricted movement of the Instrument Handle during an operation. This enhancement will increase the amount of possible cutting operations it can perform. There are many different methods of sending wireless data (i.e., WIFI and Bluetooth). These technologies are ever changing and improving, allowing the ability of these devices to become even smaller and allowing successful integration with the Instrumented Handle.

A major aspect of designing any medical device is determining the proper sterilization method. In the project, the only aspect of the sterilization method that was evaluated is the selection of 316 stainless steel commonly used in medical devices in the transducer design. Determining the proper sterilization method for the whole Instrumented Handle is still an outstanding task.

The evaluation has demonstrated that forces involved in stab and cut directions can be accurately measured with this device and the resolution and repeatability are high enough to differentiate the forces exerted between several blades interacting with different media. Therefore, this device has the ability to provide insight into the act of cutting tissue, improve the quality of surgical blades, and generate critical data necessary for creating realistic physical and

virtual training environments, it is critical to have good understanding of the biomechanical properties of tissues and the forces needed to cut tissue. Future improvement to the design system will improve measurements in the stab direction and allow for *in-vivo* testing in operating rooms.

7. References

[1] Kneebone, R.; "Simulation in Surgical Training: Educational Issues and Practical Implications." Medical Education Wiley. 2003, Volume 37, Issue 3, 267-277

[2] Balakrishnam, Asha; "Development of Novel Dynamic Indentation Techniques for Soft Tissue Application" Massachuestts Institute of Technology, Department of Mechanical Engineering, 2007, http://hdl.handle.net/1721.1/4298

[3] Rebello, K.L.; "Application of MEMS in Surgery." Proceedings of IEEE. 2004 Volume 92, Issue 1, 43-55

[4] F. J. Carter, T. G. Frank, P. J. Davies, and A. Cuschieri. "Puncture Forces of Solid Organ Surfaces." Surgical Endoscopy Springer-Verlag, New York, 2000. Volume 14, Number 9, 783-786

[5] Spataro, Joseph Edward. "Evaluation of Surgical Blade Cutting Forces." Tufts University, Department of Mechanical Engineering, 2004

[6] Brouwer, Iman; Ustin, Jeffrey; Bentley, Loren; Sherman, Alana; Dhruv, Neel; Tendick, Frank; "Measuring in Vivo Animal Soft Tissue Properties for H." Medicine Meets Virtual Reality 2001, IOS Press 2001, 69-74

[7] Okamura, Allison M.; Simone, Christina; O'Leary, Mark D.; "Force Modeling for Needle Insertion into Soft Tissue." IEEE Transactions on Biomedical Engineering. 2004, Number 10, Volume 51, 1707–1716

[8] Chanthasopeephan T.; Desai, JP,; Lau, AC,; "Study a Soft Tissue Cutting Force and Cutting Speeds." Stud Health Technol Inform. 2004, Volume 98, 56-62.

[9] Greenish, Stephanie; "Acquisition and Analysis of Cutting Force of Surgical Instruments for Haptic Simulation." McGill University, Department of Electrical and Computer Engineering, 1998

[10] Chanthasopeephan T.; Desai, JP,; Lau, AC,; "Modeling Soft-Tissue Deformation Prior to Cutting for Surgical Simulation: Finite Element Analysis and Study of Cutting Parameters." IEEE Transactions on Biomedical Engineering. 2007, Volume 54, Issue 3, 349-359